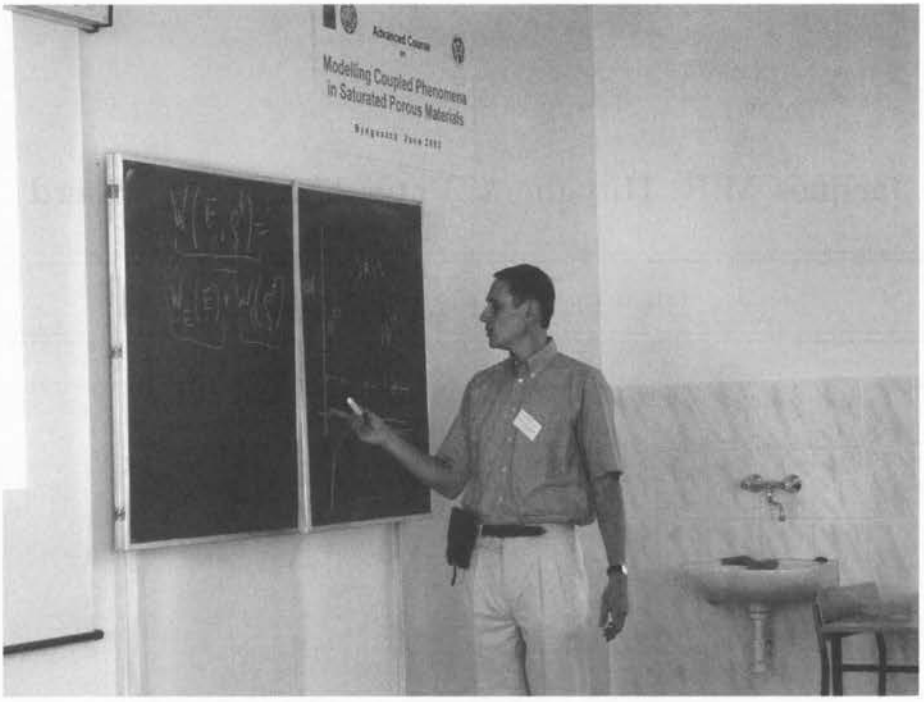

MODELLING COUPLED PHENOMENA IN SATURATED POROUS MATERIALS
POROCENT – (PP.227–276) – BYDGOSZCZ, JUNE 2003.

Biological Mixtures

J.M. Huyghe and P.H.M Bovendeerd

Technische Universiteit Eindhoven,
Faculty of Biomedical Engineering, Holland
j.m.r.huyghe@tue.nl

Coupled phenomena in porous media find increasing application in the field biology. The particular features of coupled processes that are relevant to biology and medicine are highlighted in this chapter. They are the coupling between ionization, ionic diffusion-convection, finite deformation and blood perfusion. The challenges are both in terms of deformation and blood perfusion. The challenges are both in terms of theoretical development, numerical analysis and experimental measurement. The present account focusses mostly on the theoretical framework and the numerical analysis.

Key words: *cartilage, intervertebral disc, hydrogel, ionization, finite deformation*

1. Solutions

In this section we will discuss mixtures of a liquid in which a dissolved substance, also called solutions. As an introduction we will first consider mixtures of ideal gasses. Then we will consider solutions in which the solved particles are electrically neutral: the non-electrolytic solutions. Finally we consider the electrolytic solutions, in which the solved matter falls apart in charged ions and we have to take electroneutrality into account. Particularly concepts like electrochemical potential and (Donnan) osmosis will be discussed.

Traditionally this is the field of the physical chemistry. We will follow the procedures that are usual in that field. The relations that are found here however, can also be derived from the general theory of mixtures, as we will show in section 2. The subject matter in this section has largely been taken from textbooks about physical chemistry applied to biological systems (Chang 1981, [8], Katchalsky 1965, [25], Richards 1980, [31]).

1.1. Mixtures of ideal gasses

We first consider a pure ideal gas. For a constant temperature the differential of the Gibbs free energy of the gas is :

$$dG = V dp \tag{1.1}$$

in which V is the volume of the gas and p its pressure. If we now increase the pressure of the gas from p_0 to p, the variation of the Gibbs free energy ΔG is written:

$$\Delta G = G - G_0 = \int_{G_0}^{G} dG = \int_{p_0}^{p} V dp \tag{1.2}$$

For an ideal gas applies:

$$pV = nRT \tag{1.3}$$

in which R represents the universal gas constant ($8.314\ J \cdot K^{-1} \cdot \text{mol}^{-1}$) and n is the amount of gas in moles. Substitution of (1.3) into (1.2) yields after integration:

$$G - G_0 = nRT \ln \frac{p}{p_0} \tag{1.4}$$

This equation shows the Gibbs free energy of a gas with respect to the state of reference (p_0, G_0). For the chemical potential of the gas it follows that:

$$\bar{\mu} = \bar{\mu}_0 + RT \ln \frac{p}{p_0} \tag{1.5}$$

Let's consider a *mixture of ideal gasses*. We take an amount n^I of gas I and an amount n^{II} of a gas II. Both gasses are subjected to a reference pressure p_0, and have the volumes V^I and V^{II}. During mixing of these gasses an ideal mixture with volume V and pressure p is created, for which:

$$V = V^I + V^{II} \tag{1.6}$$

$$p = p_0 \tag{1.7}$$

The *partial pressures* p^I and p^{II} of the gasses in the mixture measure:

$$p^I = x^I p_0 \qquad p^{II} = x^{II} p_0, \tag{1.8}$$

in which the molar fractions x of the components are defined as:

$$x^I = \frac{n^I}{n^I + n^{II}}, \qquad x^{II} = \frac{n^{II}}{n^I + n^{II}} \tag{1.9}$$

Substitution of the pressures from (1.8) into (1.5) now yields for the chemical potential of the gasses:

$$\bar{\mu}^I = \bar{\mu}_0^I + RT \ln x^I, \qquad \bar{\mu}^{II} = \bar{\mu}_0^{II} + RT \ln x^{II} \tag{1.10}$$

We know that the mixing process as described above occurs spontaneously. We can also see this by calculating the *mixing-energy*. The total Gibbs free energy before mixing amounts:

$$G_{voor} = n^I \bar{\mu}_0^I + n^{II} \bar{\mu}_0^{II} \tag{1.11}$$

For the total Gibbs free energy after mixing applies:

$$G_{na} = n^I \{\bar{\mu}_0^I + RT \ln x^I\} + n^{II} \{\bar{\mu}_0^{II} + RT \ln x^{II}\} \tag{1.12}$$

We can now derive for the mixture energy ΔG_{meng}:

$$\begin{aligned} \Delta G_{meng} &= G_{na} - G_{voor} \\ &= (n^I + n^{II})RT\{x^I ln x^I + x^{II} ln x^{II}\} \end{aligned} \tag{1.13}$$

Because x^I as well as x^{II} are smaller than 1, $\Delta G_{meng} < 0$, which means that the mixing process occurs indeed spontaneously.

1.2. Non-electrolytic solutions

From the former we saw that for mixtures of ideal gasses the chemical potential depends on the composition of the mixture following (1.10). In general the chemical potential for mixtures of ideal media depends on the pressure p and the temperature T. We now define an *ideal mixture* as a mixture in which the following relation applies for the chemical potential of the components α:

$$\bar{\mu}^\alpha(p, T, x^\alpha) = \bar{\mu}_0^\alpha(p, T) + RT \ln x^\alpha \tag{1.14}$$

We therefore assume that $\bar{\mu}^\alpha$ depends the same way on the composition of the mixture as a mixture of ideal gasses does. For a mixture of ideal gasses we found the concentration dependency through the partial pressures of the gasses. In definition (1.14) we take the pressure dependency separately into account in the term $\bar{\mu}_0^\alpha(p, T)$. If the mixture has an equilibrium, we know that for every component:

$$\nabla \bar{\mu}^\alpha = \mathbf{0}. \tag{1.15}$$

If all components move freely through the mixture, this means, using (1.14), that there are no gradients in concentration. If this free movement is hampered, a concentration gradient generally will be present in the equilibrium.

This last situation is demonstrated in the experiment, shown in Fig 1. In the right compartment there is a solution of n^e moles of a substance e, for example a protein, in n^w moles of a solvent w, for example water. In the solution the protein consists of neutral particles. In the left compartment only the solvent is present, water. The compartments are separated by a semi-permeable membrane, that only allows transport of water. Therefore equation 1.15 applies across the membrane for water, but not for the protein.

Initially there is no hydrostatic pressure difference between both compartments. For the chemical potential of the water applies:

$$\bar{\mu}_l^w = \bar{\mu}_0^w + RT \ln x_l^w = \bar{\mu}_0^w \quad \text{(because } x_l^w = 1\text{)} \tag{1.16}$$

$$\bar{\mu}_r^w = \bar{\mu}_0^w + RT \ln x_r^w < \bar{\mu}_0^w \quad \text{(because } x_r^w < 1\text{)} \tag{1.17}$$

in which we indicate the chemical potential of the water with $\bar{\mu}^w$, in the left (index 1) and the right (index r) compartment and in pure (index 0) state. The chemical potential of the water therefore appears to be lower on the right hand side than that on the left hand side. This difference

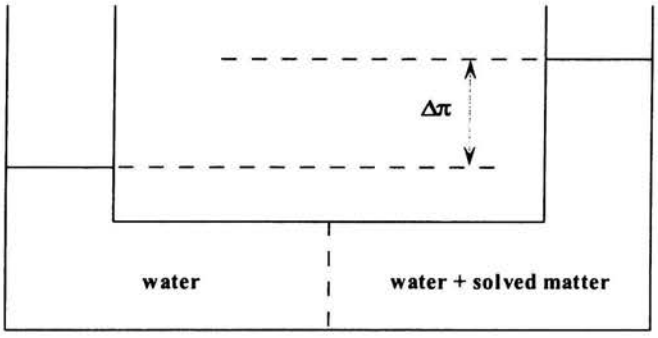

Figure 1: Illustration of the phenomenon osmotic pressure.

causes a net transport of water from the left to the right, which results in a hydrostatic pressure difference. The net transport reaches an equilibrium, as soon as the chemical potentials on the left and on the right are equal. In this equilibrium the hydrostatic pressure difference is equal to $\Delta\pi$, the *osmotic pressure difference*. We calculate the size of the osmotic pressure difference. The total differential of the Gibbs free energy G is:

$$dG = \left(\frac{\partial G}{\partial T}\right)_{p,n^\alpha} dT + \left(\frac{\partial G}{\partial p}\right)_{T,n^\alpha} dp + \sum_{\alpha=1}^{\nu} \bar{\mu}^\alpha dn^\alpha, \tag{1.18}$$

in which the chemical potential $\bar{\mu}^\alpha$ is defined as:

$$\bar{\mu}^\alpha = \bar{G}^\alpha = \left(\frac{\partial G}{\partial n^\alpha}\right)_{p,T,n^\beta,\beta\neq\alpha}. \tag{1.19}$$

We now state for the volume V and the entropy S of the mixture:

$$V = \left(\frac{\partial G}{\partial p}\right)_{T,n^\alpha} \tag{1.20}$$

$$S = -\left(\frac{\partial G}{\partial T}\right)_{p,n^\alpha} \tag{1.21}$$

The partial derivative of the chemical potential with respect to the pressure is:

$$\begin{aligned}\left(\frac{\partial \bar{\mu}^\alpha}{\partial p}\right)_{T,n^\alpha} &= \left(\frac{\partial}{\partial p}\left(\frac{\partial G}{\partial n^\alpha}\right)_{p,T,n^\beta,\beta\neq\alpha}\right)_{T,n^\alpha} \\ &= \left(\frac{\partial}{\partial n^\alpha}\left(\frac{\partial G}{\partial p}\right)_{T,n^\alpha}\right)_{p,T,n^\beta,\beta\neq\alpha},\end{aligned} \tag{1.22}$$

which can be rewritten, using (1.20), into:

$$\left(\frac{\partial \bar{\mu}^\alpha}{\partial p}\right)_{T,n^\alpha} = \left(\frac{\partial V}{\partial n^\alpha}\right)_{T,p,n^\beta,\beta\neq\alpha} = \bar{V}^\alpha \tag{1.23}$$

in which $\bar{V}^\alpha$ is the partial molar volume of the component α in the mixture. Applied to the water-component in the situation of Fig. 1, we find:

$$\left(\frac{\partial \bar{\mu}^w}{\partial p}\right)_{T,n^w,n^e} = \bar{V}^w = \bar{V}_0^w \tag{1.24}$$

The last '='-sign can be justified for a *dilute solution*, in which the partial molar volume of the water is equal to that of pure water. We determine the difference in chemical potential of the water in both compartments, as a result of the pressure difference $p_r - p_l$, through integration of (1.24), considering that the partial molar volume of the water is independent of the pressure:

$$\bar{\mu}_r^w - \bar{\mu}_l^w = \int_{p_l}^{p_r} \bar{V}_0^w dp = \bar{V}_0^w (p_r - p_l) \tag{1.25}$$

In equilibrium the chemical potential of the water left and right is the same:

$$\bar{\mu}_l^w = \bar{\mu}_r^w = \bar{\mu}_0^w + RT \ln x_r^w + \bar{V}_0^w (p_r - p_l) \tag{1.26}$$

Because $\bar{\mu}_l^w = \bar{\mu}_0^w$, the osmotic pressure difference $\Delta\pi$ is:

$$\Delta\pi = p_r - p_l = -\frac{RT}{\bar{V}_0^w} \ln x_r^w \tag{1.27}$$

It is usual to relate the osmotic pressure to the concentration of the solution, the protein. For this, we use:

$$\ln x^w = \ln(1 - x^e) \approx -x^e = -\frac{n^e}{n^w + n^e} \approx -\frac{n^e}{n^w} \tag{1.28}$$

and the following expression for the volume V of the solution:

$$V = n^w \bar{V}^w + n^e \bar{V}^e \approx n^w \bar{V}_0^w. \tag{1.29}$$

Substitution of these relations in (1.27) yields:

$$\Delta\pi = \frac{n^e}{V} RT = c^e RT, \tag{1.30}$$

in which the *concentration* c^e is expressed in moles·m^{-3}. This relation has also been discovered empirically by *Van't Hoff*, indicating that the basic assumption for an ideal mixture, defined in (1.14), applies for dilute solutions. We define the osmotic pressure of a solution as:

$$\pi = -\frac{RT}{\bar{V}_0^w} \ln x^w, \tag{1.31}$$

which is well approximated by van 't Hoff's equation in a dilute solution:

$$\pi = c\, RT. \tag{1.32}$$

in which c is the concentration of the solved substances. Further, we specify expression (1.14) for the chemical potential of a component α, using (1.26):

$$\bar{\mu}^\alpha = \bar{\mu}_0^\alpha(T) + RT \ln x^\alpha + p\bar{V}^\alpha. \tag{1.33}$$

with particularly for water:

$$\bar{\mu}^w = \bar{\mu}_0^w(T) + RT \ln x^w + \bar{V}_0^w p = \bar{\mu}_0^w(T) + \bar{V}_0^w(p - \pi) \tag{1.34}$$

In other words, the chemical potential consists of a pressure dependent part (the pressure potential) and a concentration-dependent part (the osmotic potential) for isothermal conditions. Deviations of the ideal situations are taken into account using the so called *activity coefficient* γ^α. The molar fraction x^α is corrected to an 'active molar fraction', or *activity* a^α:

$$a^\alpha = \gamma^\alpha x^\alpha, \tag{1.35}$$

The expression for the chemical potential then becomes:

$$\bar{\mu}^\alpha = \bar{\mu}_0^\alpha(T) + RT \ln a^\alpha + p\bar{V}^\alpha. \tag{1.36}$$

1.3. Electrolytic solutions

In biology we often have to deal with solutions of ionized high-molecular proteins. In this paragraph we will consider solutions of a protein, (component e) and a low-molecular salt (component z) in water (component w). We will indicate the protein with PX_z. We assume that in a solution of this protein an equilibrium will be established in which a protein molecule falls apart in a high molecular negative ion P^{z-} and z small positive ions X^+:

$$PX_z \rightleftharpoons P^{z-} + zX^+. \tag{1.37}$$

In general there are also ions present of a low-molecular electrolyte in such a protein solution, indicated with MZ. We assume that a solution of this electrolyte results in monovalent positive and negative ions:

$$MX \rightleftharpoons M^- + X^+. \tag{1.38}$$

In this situation the M^-- and the X^+-ion are called the 'co-ion' and the 'counter-ion' respectively.

Since the time constant, corresponding to the establishment of a local electrostatic equilibrium, is very short, we can assume that at every moment electroneutrality applies.

1.3.1. The electrochemical potential of an ionic component

In the former the chemical potential of a component α was defined as the partial molar Gibbs free energy. This means that we considered the change of the Gibbs free energy if we added one mole of component α to the mixture, during which we kept the amounts of the other components constant. For a solution of an electrolyte, for example the salt MZ, the movement of cations or anions is not exclusively controlled by the chemical potential, as was the case for the water in the porous medium [19]. Reason for this is, that the charged particle is also sensitive for an electric-potential field. One mole of a monovalent ion has a charge equal to the constant of Faraday, F. The force that works on an ion in an electric-potential field ξ is:

$$F\nabla\xi \tag{1.39}$$

Therefore, we do not use the chemical potential for an ionic component but the electro-chemical potential, of which the gradient does not only contain

the mechanical and chemical forces, but also the electric forces:

$$\bar{\mu}^{\alpha} = \bar{\mu}_0^{\alpha} + RTlna^{\alpha} + p\bar{V}^{\alpha} + z^{\alpha}F\xi \quad \alpha = +, - \tag{1.40}$$

Here, z^{α} is the valence of the ion, from which it follows that for a salt in water the chemical potential is:

$$\bar{\mu}^{z} = \bar{\mu}_0^{z} + RT \ln a^{z} + p\bar{V}^{z}, \tag{1.41}$$

We see that the *activity of the salt* is,

$$a^{z} = a^{+}a^{-}, \tag{1.42}$$

that the reference-potential is,

$$\bar{\mu}_0^{z} = \bar{\mu}_0^{+} + \bar{\mu}_0^{-}, \tag{1.43}$$

and that the partial molar volume is,

$$\bar{V}^{z} = \bar{V}^{+} + \bar{V}^{-}. \tag{1.44}$$

We now define the activity coefficients for the ions γ^{+} and γ^{-}, in analogy to (1.35), as:

$$a^{+} = \gamma^{+}x^{+}, \qquad a^{-} = \gamma^{-}x^{-}, \tag{1.45}$$

in which x^{+} and x^{-} represent the (equal) molar fractions of the anion and the cation. We can now derive the activity of the salt a^{z}:

$$a^{z} = \gamma^{+}x^{+}\gamma^{-}x^{-} = (\gamma^{\pm}x)^{2}, \tag{1.46}$$

in which we defined the *average activity coefficient* of the salt $\gamma^{\pm}$ as:

$$\gamma^{\pm} = (\gamma^{+}\gamma^{-})^{1/2}, \tag{1.47}$$

and used $x^{+} = x^{-} = x$. The activity coefficients can be determined experimentally from electro-chemical experiments. A theoretical foundation of the relations above is provided for strongly diluted solutions by Debye and Hückel in 1923. In this course we consider the relations as empirical ones. It is obvious that the relations for the chemical potential of a salt as mentioned above do not apply for a pair of ions, present in a porous medium with fixed charges, because in that case the co-ionic charge and the counter-ionic charge do not neutralize one another and therefore one cannot speak of a salt (=electric neutral molecule) in a solution.

1.3.2. The Donnan-effect

The Donnan-effect occurs in a saturated electrically charged porous solid. We consider two neighbouring points in the charged porous medium. Between these two points there is a difference in fixed charge concentration. The two points are now considered to be two containers, between which water and ions (M^- en X^+) can move freely. The fixed charges (P^{z-}), however, cannot move from one container to the other. In other words, the containers communicate through a semi-permeable medium (Fig. 2). To fix our thoughts and without

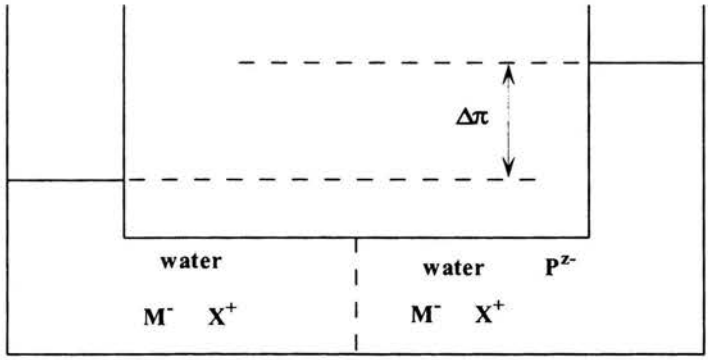

Figure 2: Illustration of the Donnan-effect.

loss of generality, we assume that the left container has no fixed charge. An equilibrium is established, in which no net transport of particles through the membrane takes place. This equilibrium is characterized by the condition, that the (electro)-chemical potential for substances, that are able to pass the medium freely, is equal in the left as well as the right container:

$$\bar{\mu}_l^w = \bar{\mu}_r^w \tag{1.48}$$

$$\bar{\mu}_l^\alpha = \bar{\mu}_r^\alpha \quad \alpha = +, - \tag{1.49}$$

Using (1.36) we can write these relations as:

$$\bar{\mu}_0^w + RT \ln a_l^w + p_l \bar{V}^w = \bar{\mu}_0^w + RT \ln a_r^w + p_r \bar{V}^w, \tag{1.50}$$

$$\bar{\mu}_0^\alpha + RT \ln a_l^\alpha + p_l \bar{V}^\alpha + z^\alpha F \xi_l = \bar{\mu}_0^\alpha + RT \ln a_r^\alpha + p_r \bar{V}^\alpha + z^\alpha F \xi_r \quad \alpha = +, -. \tag{1.51}$$

Now, we first consider the ionic equilibrium. As the solution is dilute, the contribution $p\bar{V}^\alpha$ is negligible with respect to the term $RT \ln a^\alpha$. With this

the summation of (1.51), for $\alpha = +, -$, reduces to the condition:

$$a_l^+ a_l^- = a_r^+ a_r^- \tag{1.52}$$

Using (1.46) this leads, after conversion to concentrations, to:

$$(\gamma^\pm)_l^2 c_l^+ c_l^- = (\gamma^\pm)_r^2 c_r^+ c_r^- \tag{1.53}$$

Beside this condition, the condition of electroneutrality for the solution in the left as well as the right compartment should be kept. Deviation from electroneutrality would lead to - relative strong - electric forces, restoring electroneutrality almost immediately. Therefore:

$$c_l^+ = c_l^- \tag{1.54}$$

$$c_r^+ = c_r^- + z c_r^e, \tag{1.55}$$

in which c^e is the concentration of the macromolecule to which z fixed charges are attached. For the concentrations of M^-- and X^+-ions in the left and right compartment a combination of (1.53) – (1.55) yields:

$$c_r^- = \frac{1}{2}\left(z c_r^e + \sqrt{(z c_r^e)^2 + \frac{(\gamma_l^\pm)^2 (c_l^-)^2}{(\gamma_r^\pm)^2}} \right) \tag{1.56}$$

$$c_r^- = \frac{1}{2}\left(-z c_r^e + \sqrt{(z c_r^e)^2 + \frac{(\gamma_l^\pm)^2 (c_l^-)^2}{(\gamma_r^\pm)^2}} \right) \tag{1.57}$$

In a dilute solution we are allowed to equate the activity coefficients $\gamma_l^\pm$ and $\gamma_r^\pm$. We now see that the concentration c^+ of the X^+-ions is different between left and right, as is the concentration c^- of the M^--ions. This difference in concentration is called the *Donnan-effect*. We also see, that the Donnan-effect decreases for an increasing salt concentration.

The osmotic pressure difference between the left and the right compartment $\Delta\pi$ can now be determined from the equilibrium for the water. Therefore, we rewrite (1.51) as:

$$\Delta\pi = p_r - p_l = -\frac{RT}{\bar{V}^w} \ln \frac{a_r^w}{a_l^w}, \tag{1.58}$$

If we suppose that the activity coefficients for water are equal left and right, we can switch to molar fractions:

$$x_l^w = \frac{c_l^w}{c_l^w + c_l^+ + c_l^-} = 1 - \frac{c_l^+ + c_l^-}{c_l^w + c_l^+ + c_l^-} \tag{1.59}$$

$$x_r^w = \frac{c_r^w}{c_r^w + c_r^+ + c_r^- + c_r^e} = 1 - \frac{c_r^+ + c_r^- + c_r^e}{c_r^w + c_r^+ + c_r^- + c_r^e} \tag{1.60}$$

Because the water concentration is much higher than the other concentrations, we can use the first order approximation $\ln(1+x) \approx x$ and we will find:

$$\frac{\Delta\pi \bar{V}^w}{RT} = \frac{c_r^+ + c_r^- + c_r^e}{c_r^w} - \frac{c_l^+ + c_l^-}{c_l^w}, \tag{1.61}$$

This expression can be simplified further, because $c_l^w \approx c_r^w = 1/\bar{V}^w \approx 1/\bar{V}_0^w$, which gives:

$$\Delta\pi = RT(c_r^+ - c_l^+ + c_r^- - c_l^- + c_r^e) \tag{1.62}$$

In many cases the valence z of the protein is very high and therefore the contribution of the protein concentration c^e is neglectable, compared to the concentrations of the small ions. If we define the osmotic pressure, in this case, as:

$$\pi = RT(c^+ + c^-) \tag{1.63}$$

we find the former expression for the osmotic pressure difference back. In the non-ideal situation equation 1.63 is extended with an osmotic coefficient Γ:

$$\pi = \Gamma RT(c^+ + c^-) \tag{1.64}$$

From equation (1.51) also the Donnan-potential difference between the left and right compartment follows:

$$\xi_r - \xi_l = \frac{RT}{F} ln \frac{a_l^+}{a_r^+} = \frac{RT}{F} ln \frac{a_r^-}{a_l^-} \tag{1.65}$$

1.3.3. Donnan osmosis in biological tissues

The semi-permeable membrane exists in many forms in nature: for example as a cell membrane, as a layer endothelial cells (covering the inner side of blood vessels), or as elastic lamina (a layer that is found in the wall of arteries). The transmembrane potential observed across the membrane of a living cell is a Donnan-potential. However, one should realize that many biological

tissues function as a semipermeable medium leading to the Donnan-effect (and to osmosis) as a continuous osmotic pressure gradient across the tissue. Therefore the Donnan-effect occurs in, for example, cartilage, where the huge, ionized proteoglycan molecules are tangled in a network of collagen and elastine fibers. The charge of the proteoglycan molecules is caused by the negative carboxyl groups (COO^-) and sulphate groups (SO_3^-). It will be clear from the former, that not the concentration of big molecules c^e, but the concentration of negatively combined charge zc^e, is an important characteristic quantity of the material. This concentration is often called *fixed charge density* c^{fc}. We come across several small ions in biological tissues like Na^+, K^+, Ca^{2+} en Cl^-.

For studying the properties of biological tissues, synthetic model materials are developed, consisting of ionised polymer chains (de Heus, 1994). The Donnan-osmotic effect can be used to determine the fixed charge density c^{fc} in these materials. The model material ('the right compartment') is therefore exposed to an external solution of a known concentration ('the left compartment'), after which the osmotic pressure in the material is measured. In Fig. 3 the measured osmotic pressure is plotted against the external salt concentration. From a combination of the relations (1.53) – (1.57) and (1.62)

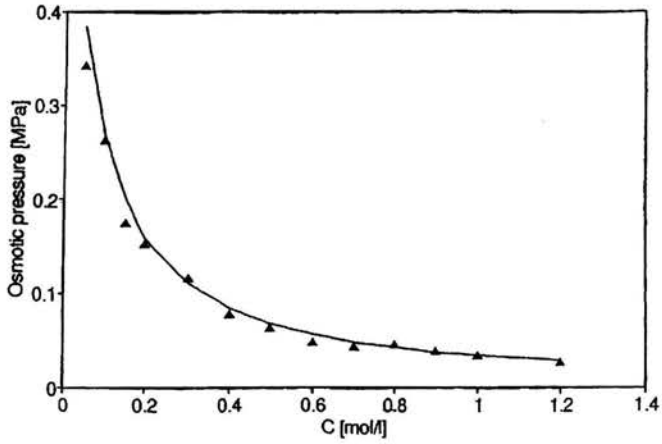

Figure 3: Measured relation between the osmotic pressure and external salt concentration (△) in a synthetic material. The drawn line represents relation (1.67), with parameter values $\Phi = \Phi^* = 0.93$, $f = 1$ and $c^{fc} = 0.24 \cdot 10^3 \text{mol} \cdot \text{m}^{-3}$.

we can eliminate the concentration of free ions in the model material, which

will result in:

$$\Delta\pi = RT\{c^{fc^2} + 4f^2c^2\}^{1/2} - 2cRT, \tag{1.66}$$

in which $c = c_l^+ = c_l^-$ is the (known) concentration of ions in the external solution, and f is a short notation for the relation between the activity of salt in the external solution and that in the material $f = \gamma_l^{\pm}/\gamma_r^{\pm}$. We have to realize, that several approximations have been introduced when deriving expression (1.62). A more elaborate derivation leads to:

$$\Delta\pi = \Phi RT(c^{fc^2} + 4f^2c^2)^{1/2} - 2\Phi^* cRT, \tag{1.67}$$

with *osmotic coefficients* Φ and Φ^*. The unknowns in this relation can be determined by fitting the experimental data. From Fig. 3, we see that the relation between the measured concentration and the osmotic pressure can be described well using relation (1.67).

1.4. Chemical potential and mass transport

In the former it is stated, that the direction in which thermodynamic processes go, is dependent of differences in chemical potential. We will now specify this statement for the flow of a dissolved substance in a solution. The 'derivation' is meant to give better insight and not to be mathematically precise.

As an introduction we consider a simple one dimensional system, characterized by a mass m and a friction coefficient k, to which a force $\boldsymbol{f}$ is applied, that is related to a potential $\bar{\mu}$. The system model for such a system reads:

$$\boldsymbol{f} = \boldsymbol{\nabla}\bar{\mu} = m\boldsymbol{a} + k\boldsymbol{v}, \tag{1.68}$$

in which $\boldsymbol{v}$ and $\boldsymbol{a}$ are the velocity and the acceleration of the system. Some time after the force is applied to the system a stationary state will be established, in which the acceleration equals zero, so the velocity $\boldsymbol{v}$ is proportional to the gradient of the potential $\bar{\mu}$:

$$\boldsymbol{v} = \frac{1}{k}\boldsymbol{\nabla}\bar{\mu} \tag{1.69}$$

Similarly the flow of a constituent α in a solution can also be considered. If we state again, that the friction term is linear in velocity, we find:

$$\boldsymbol{v}^\alpha = \boldsymbol{L}^\alpha \cdot \boldsymbol{\nabla}\bar{\mu}^\alpha, \tag{1.70}$$

in which $\boldsymbol{L}^{\alpha}$ is a second order tensor. Substitution of expression (1.33) for the chemical potential yields:

$$\boldsymbol{v}^{\alpha} = \boldsymbol{D}^{\alpha} \cdot \boldsymbol{\nabla} x^{\alpha} + \boldsymbol{K}^{\alpha} \cdot \boldsymbol{\nabla} p \tag{1.71}$$

If a pressure gradient is absent, we recognize the *law of Fick* for diffusion of constituents caused by a concentration gradient. In the absence of a concentration gradient the equation reduces to the *law of Darcy* for flow of a fluid through a porous medium caused by the influence of a pressure gradient. The tensor $\boldsymbol{K}^{\alpha}$ therefore represents a *permeability tensor*, while $\boldsymbol{D}^{\alpha}$ is a *diffusion tensor*. If we deal with an isotropic system, these tensors reduce to $K^{\alpha}\,\boldsymbol{I}$ and $D^{\alpha}\,\boldsymbol{I}$, respectively.

Questions

1. What is the osmotic pressure of a physiological ionic solution?
2. A piece of cartilage has a fixed charge density c^{fc} of 0.1 moleq/l, a porosity of 0.7, a Young's modulus of 100 kPa and a Poisson's ratio of 0.3. These values are measured for an equilibrium with a 0.2 mol/l NaCl solution. The sample is put in a 0.15 mol/l NaCl solution. What is the volumetric swelling of the sample? Consider all activity coefficients equal to 1.

2. Quadriphasic mixture theory: A gel model of tissue

Since antiquity swelling has been known as a primary symptom of disease. This deals deals with finite deformation theory of a four-component mixture. The four components are : an electrically charged solid, a fluid, and a cationic and anionic component. The model is suitable to describe time-dependent deformation of gellike tissues including swelling.

2.1. Introduction

In [19] we presented a biphasic model of biological tissue. This model basically assumes that the tissue is a sponge saturated with a viscous fluid. Anyone who has worked with biological tissue will agree there is something realistic about this, although many body fluids look more like a gel than a fluid. This is true, e.g., for intracellular fluid, interstitial fluid and for synovial fluid. Part of those fluids are bound by hygroscopic macromolecules and are not free to move as assumed in biphasic mixture theory. Cartilaginous tissue is a tissue in which this gel property is dramatic. The pressure in the intervertebral disk of an unloaded spine, e.g., exceeds 0.1 MPa showing that strong forces are attracting fluid in the disk. If the disks of the spine were biphasic, they would very soon loose their fluid content (= 60 to 90 % of their volume), cause the spine to shorten under its daily load and be unable to perform their function. In fact hygroscopic macromolecular networks ensure that the fluid component of biological tissue remains under compression and the fibrous solid remains under tension irrespective of the loads applied on the tissue. The functionality of this lies in the inability of fibers to take up compression and the fluid to take up uni- or biaxial tensile loads. The physiological relevance of the hydrophylic nature of the solid component of biological tissues is clearly illustrated by the close correlation between water content of the human body and age. Maintenance of youthfulness is closely associated with the maintenance of hydrophylic

nature of macromolecular networks within the tissue. Smoothness of skin is achieved by tensile prestressing the skin. Loss of fluid content of cutaneous and subcutaneous structures necessarily implies wrinkling of the skin. The load bearing capacity of cartilage strongly depends on the gellike fluid inside the cartilage layer to transform the compressive load into a tensile fibre stress. In the literature, finite deformation formulations are found in [17] in the isothermal case, in [18] in the non-isothermal case, in [14] for a dual porosity model. Some experimental work aiming at verifying some aspects of the theory are found in [10] for intervertebral disk, in [26] for hydrogel, in [15] for a dual porosity model of intervertebral disk in [16, 20] for electro-osmosis experiments. An efficient numerical scheme to deal with isothermal finite deformation of single porosity gels is give by [37].

2.2. Basic assumptions

We distinguish a solid (superscript s), a fluid (superscript f) , a cationic component (superscript $+$) and an anionic component (superscript $-$). As is usual in porous media mechanics we consider trapped fluid (e.g. intracellular fluid) to belong to the solid because the fluid is not free to move. Part of the solid is assumed to be ionized. In case of cartilage or intervertebral disk this might be the proteoglycan network which is negatively charged (they contain COO^- en SO_3^-). The fixed charge density c^{fc} is expressed per unit volume of fluid. The cationic component is assumed to consist of only one monovalent cation (e.g. Na^+) with molar mass M^+, molar volume $\bar{V}^+$ and concentration c^+ per unit fluid volume. The anionic component is assumed to consist of only one monovalent anion (e.g. Cl^-) with molar mass M^-, molar volume $\bar{V}^-$ and concentration c^- per unit fluid volume. We assume all phases intrinsically incompressible, i.e. the intrinsic density

$$\rho_i^\alpha = \frac{\rho^\alpha}{\phi^\alpha}, \qquad \alpha = s, f, +, - \tag{2.1}$$

is constant.

2.3. Conservation laws

Excluding mass transfer between phases, the mass balance of each phase is then written as:

$$\frac{\partial \phi^\alpha}{\partial t} + \boldsymbol{\nabla} \cdot (\phi^\alpha \boldsymbol{v}^\alpha) = 0, \qquad \alpha = s, f, +, - \tag{2.2}$$

in which ϕ^α is the volume fraction and $\boldsymbol{v}^\alpha$ the velocity of phase α. As we assume saturation, we find

$$\phi^s + \phi^f + \phi^+ + \phi^- = 1 \tag{2.3}$$

Differentiation of equation (2.3) and substitution of the mass balance equations (2.2) yields the differentiated from of the saturation condition:

$$\boldsymbol{\nabla} \cdot \boldsymbol{v}^s + \sum_{\beta=f,+,-} \boldsymbol{\nabla} \cdot \left(\phi^\beta (\boldsymbol{v}^\beta - \boldsymbol{v}^s) \right) = 0 \tag{2.4}$$

We refer current descriptors of the mixture with respect to an initial state of the porous solid. If we introduce volume fractions

$$\Phi^\alpha = J\phi^\alpha \tag{2.5}$$

per unit initial volume, we can rewrite the mass balance equation (2.2) as follows:

$$\frac{D^s \Phi^\alpha}{Dt} + J\boldsymbol{\nabla} \cdot [\phi^\alpha (\boldsymbol{v}^\alpha - \boldsymbol{v}^s)] = 0 \tag{2.6}$$

The electroneutrality condition requires :

$$C^- = C^+ + C^{fc} \tag{2.7}$$

in which C^β is the current molar concentration per unit initial mixture volume:

$$C^\beta = J\phi^f c^\beta \quad \beta = +, -, fc \tag{2.8}$$

As the fixed charges are linked to the solid, we know that

$$\frac{D^s C^{fc}}{Dt} = 0 \tag{2.9}$$

Differentiation of (2.7) with respect to time yields:

$$\frac{D^s C^-}{Dt} = \frac{D^s C^+}{Dt} \tag{2.10}$$

or, after substitution of eq. (2.6),

$$\frac{1}{V^+} \boldsymbol{\nabla} \cdot [\phi^+ (\boldsymbol{v}^+ - \boldsymbol{v}^s)] = \frac{1}{V^-} \boldsymbol{\nabla} \cdot [\phi^- (\boldsymbol{v}^- - \boldsymbol{v}^s)] \tag{2.11}$$

in which $\overline{V}^{\beta}$ are the partial molar volumes of the ions.Neglecting body forces and inertia, the momentum balance takes the form:

$$\nabla \cdot \boldsymbol{\sigma}^{\alpha} + \boldsymbol{\pi}^{\alpha} = \mathbf{0}, \qquad \alpha = s, f, +, - \tag{2.12}$$

which after summation over the four phases, yields:

$$\nabla \cdot \boldsymbol{\sigma} = \nabla \cdot \boldsymbol{\sigma}^{s} + \nabla \cdot \boldsymbol{\sigma}^{f} + \nabla \cdot \boldsymbol{\sigma}^{+} + \nabla \cdot \boldsymbol{\sigma}^{-} = \mathbf{0} \tag{2.13}$$

if use is made of the balance condition:

$$\boldsymbol{\pi}^{s} + \boldsymbol{\pi}^{f} + \boldsymbol{\pi}^{+} + \boldsymbol{\pi}^{-} = \mathbf{0} \tag{2.14}$$

$\boldsymbol{\sigma}^{\alpha}$ is the partial stress tensor of constituent α, $\boldsymbol{\pi}^{\alpha}$ is the momentum interaction with constituents other than α. Balance of moment of momentum requires that the stress tensor $\boldsymbol{\sigma}$ be symmetric. If no moment of momentum interaction between components occurs, the partial stresses $\boldsymbol{\sigma}^{\alpha}$ also are symmetric. In this paper we assume all partial stresses to be symmetric. Under isothermal and incompressible conditions, the entropy inequality for a unit volume of mixture reads:

$$\sum_{\alpha=s,f,+,-} \left(-\phi^{\alpha} \frac{D^{\alpha}\Psi^{\alpha}}{Dt} + \boldsymbol{\sigma}^{\alpha} : \boldsymbol{D}^{\alpha} - \boldsymbol{\pi}^{\alpha} \cdot \boldsymbol{v}^{\alpha} \right) \geq 0. \tag{2.15}$$

in which Ψ^{α} is the Helmholtz free energy of constituent α per unit volume constituent. We introduce the strain energy function

$$W = J \sum_{\alpha=s,f,+,-} \phi^{\alpha}\Psi^{\alpha} = J \sum_{\alpha=s,f,+,-} \psi^{\alpha} \tag{2.16}$$

as the Helmholtz free energy of a mixture volume which in the *initial* state of the solid equals unity. ψ^{α} is the Helmholz free energy of constituent α per unit mixture volume. Rewriting the inequality (2.15) for the entropy production per initial mixture volume - i.e. we multiply inequality (2.15) by the relative volume change J - we find:

$$\begin{aligned} &-\frac{D^{s}}{Dt}W + J\boldsymbol{\sigma} : \nabla \boldsymbol{v}^{s} \\ &+J\nabla \cdot \sum_{\beta=f,+,-} [(\boldsymbol{v}^{\beta} - \boldsymbol{v}^{s}) \cdot \boldsymbol{\sigma}^{\beta} - (\boldsymbol{v}^{\beta} - \boldsymbol{v}^{s})\psi^{\beta}] \geq 0. \end{aligned} \tag{2.17}$$

The entropy inequality should hold for an arbitrary state of the mixture, complying with the balance laws, incompressibility, saturation and

electroneutrality. There are two ways to comply with these restrictions. One is substitution of the restriction into the inequality, resulting in elimination of a field variable. The other is by introduction of a Lagrange multiplier. The balance laws and the incompressibility condition (2.1) are accounted for by means of substitution. The differentiated forms of the saturation condition (2.4) and of the electroneutrality (2.11) are accounted for by means of a Lagrange multiplier. From the inequality 2.17 we see that the apparent density and the momentum interaction π is already eliminated from the inequality. In other words the conditions of incompressibility and the momentum balance have already been substituted into the second law. Therefore, restrictions still be fulfilled are the mass balances, saturation and the electroneutrality. The differentiated form of the saturation condition (2.4) is substituted by means of a Lagrange multiplier p:

$$
\begin{aligned}
&-\frac{D^s}{Dt}W + J\boldsymbol{\sigma}^{eff} : \boldsymbol{\nabla}\boldsymbol{v}^s \\
&+J\sum_{\beta=f,+,-}[\boldsymbol{\sigma}^\beta + (p\phi^\beta - \psi^\beta)\boldsymbol{I}] : \boldsymbol{\nabla}(\boldsymbol{v}^\beta - \boldsymbol{v}^s) \\
&+J\sum_{\beta=f,+,-}(\boldsymbol{v}^\beta - \boldsymbol{v}^s)\cdot(-\boldsymbol{\nabla}\psi^\beta + p\boldsymbol{\nabla}\phi^\beta + \boldsymbol{\nabla}\cdot\boldsymbol{\sigma}^\beta) \geq 0. \qquad (2.18)
\end{aligned}
$$

in which the effective stress $\boldsymbol{\sigma}^{eff}$ is defined as

$$
\boldsymbol{\sigma}^{eff} = \boldsymbol{\sigma} + p\boldsymbol{I} \qquad (2.19)
$$

Introducing the restriction (2.11) into inequality (2.18) by means of a Lagrange multiplier λ, yields:

$$
\begin{aligned}
&-\frac{D^s}{Dt}W + J\boldsymbol{\sigma}^{eff} : \boldsymbol{\nabla}\boldsymbol{v}^s \\
&+J\sum_{\beta=f,+,-}[\boldsymbol{\sigma}^\beta + ((p + \frac{z^\beta\lambda}{\overline{V}^\beta})\phi^\beta - \psi^\beta)\boldsymbol{I}] : \boldsymbol{\nabla}(\boldsymbol{v}^\beta - \boldsymbol{v}^s) \\
&+J\sum_{\beta=f,+,-}(\boldsymbol{v}^\beta - \boldsymbol{v}^s)\cdot \\
&[-\boldsymbol{\nabla}\psi^\beta + (p + \frac{z^\beta\lambda}{\overline{V}^\beta})\boldsymbol{\nabla}\phi^\beta + \boldsymbol{\nabla}\cdot\boldsymbol{\sigma}^\beta] \geq 0. \qquad (2.20)
\end{aligned}
$$

in which z^β is the valence of constituent β. We choose as independent variables the Green strain $\boldsymbol{E}$, the Lagrangian form of the volume fractions of

the fluid and the ions Φ^β, and of the relative velocities $\boldsymbol{v}^{\beta s} = \boldsymbol{F}^{-1} \cdot (\boldsymbol{v}^\beta - \boldsymbol{v}^s)$, $\beta = f, +, -$. We apply the principle of equipresence, i.e. all dependent variables depend on all independent variables, unless the entropy inequality requires otherwise. We apply the chain rule for time differentiation of W:

$$\begin{aligned}
&(J\boldsymbol{\sigma}^{eff} - \boldsymbol{F} \cdot \frac{\partial W}{\partial \boldsymbol{E}} \cdot \boldsymbol{F}^c) : \boldsymbol{\nabla} \boldsymbol{v}^s + \\
&\sum_{\beta=f,+,-} \{ \frac{\partial W}{\partial \boldsymbol{v}^{\beta s}} \cdot \frac{D^s}{Dt} \boldsymbol{v}^{\beta s} \\
&+ J[\boldsymbol{\sigma}^\beta + (\mu^\beta \phi^\beta - \psi^\beta) \boldsymbol{I}] : \boldsymbol{\nabla}(\boldsymbol{v}^\beta - \boldsymbol{v}^s) \\
&+ J(\boldsymbol{v}^\beta - \boldsymbol{v}^s) \cdot (-\boldsymbol{\nabla} \psi^\beta + \mu^\beta \boldsymbol{\nabla} \phi^\beta + \boldsymbol{\nabla} \cdot \boldsymbol{\sigma}^\beta) \} \geq 0.
\end{aligned} \tag{2.21}$$

in which μ^β are the electrochemical potentials of fluid and ions:

$$\begin{aligned}
\mu^f &= \frac{\partial W}{\partial \Phi^f} + p \\
\mu^+ &= \frac{\partial W}{\partial \Phi^+} + p + \frac{\lambda}{V^+} \\
\mu^- &= \frac{\partial W}{\partial \Phi^-} + p - \frac{\lambda}{V^-}
\end{aligned} \tag{2.22}$$

Comparison of the above equations to the classical equations of electrochemistry (1.36-1.40) indicates that the Lagrange multiplier p can be interpreted as the fluid pressure and λ as the electrical potential of the medium multiplied by the constant of Faraday. Eq. (2.21) should be true for any value of the state variables. Close inspection of the choice of independent variables and the inequality (2.21), reveals that the first term of (2.21) is linear in the solid velocity gradient $\boldsymbol{\nabla} \boldsymbol{v}^s$, the second term linear in $\frac{D^s}{Dt} \boldsymbol{v}^{\beta s}$ and the third term linear in the relative velocity gradients $\boldsymbol{\nabla}(\boldsymbol{v}^\beta - \boldsymbol{v}^s)$. Therefore, by a standard argument, we find:

$$\boldsymbol{\sigma}^{eff} = \frac{1}{J} \boldsymbol{F} \cdot \frac{\partial W}{\partial \boldsymbol{E}} \cdot \boldsymbol{F}^c \tag{2.23}$$

$$\frac{\partial W}{\partial \boldsymbol{v}^{\beta s}} = \boldsymbol{0} \tag{2.24}$$

$$\boldsymbol{\sigma}^\beta = (\psi^\beta - \mu^\beta \phi^\beta) \boldsymbol{I} \tag{2.25}$$

leaving as inequality:

$$\sum_{\beta=f,+,-} J(\boldsymbol{v}^\beta - \boldsymbol{v}^s) \cdot (-\boldsymbol{\nabla} \psi^\beta + \mu^\beta \boldsymbol{\nabla} \phi^\beta + \boldsymbol{\nabla} \cdot \boldsymbol{\sigma}^\beta) \geq 0. \tag{2.26}$$

Eq. (2.23) indicates that the effective stress of the mixture can be derived from a strain energy function W which represents the free energy of the mixture. Eq. (2.24) shows that the strain energy function cannot depend on the relative velocities. Thus, the effective stress of a quadriphasic medium can be derived from a regular strain energy function, which physically has the same meaning as in single phase or biphasic media, but which can depend on both strain and ion concentrations in the medium. According to eq. (2.25) the partial stress of the fluid and the ions are scalars. Transforming the relative velocities to their Lagrangian equivalents, we find in stead of (2.26):

$$\sum_{\beta=f,+,-} \boldsymbol{v}^{\beta s} \cdot [-\boldsymbol{\nabla}_0 \psi^\beta + \mu^\beta \boldsymbol{\nabla}_0 \phi^\beta + \boldsymbol{\nabla}_0 \cdot \boldsymbol{\sigma}^\beta] \geq 0. \tag{2.27}$$

in which $\boldsymbol{\nabla}_0 = \boldsymbol{F}^c \cdot \boldsymbol{\nabla}$ is the gradient operator with respect to the initial configuration. If we assume that the system is not too far from equilibrium, we can express the dissipation (2.27) associated with relative flow of fluid and ions as a quadratic function of the relative velocities:

$$-\boldsymbol{\nabla}_0 \psi^\beta + \mu^\beta \boldsymbol{\nabla}_0 \phi^\beta + \boldsymbol{\nabla}_0 \cdot \boldsymbol{\sigma}^\beta = \sum_{\gamma=f,+,-} \boldsymbol{B}^{\beta\gamma} \cdot \boldsymbol{v}^{\gamma s} \tag{2.28}$$

$\boldsymbol{B}^{\beta\gamma}$ is a positive definite matrix of frictional coefficients. Substituting eq. (2.25) into eq. (2.28) yields Lagrangian forms of the classical equations of irreversible thermodynamics:

$$-\phi^\beta \boldsymbol{\nabla}_0 \mu^\beta = \sum_{\gamma=f,+,-} \boldsymbol{B}^{\beta\gamma} \cdot \boldsymbol{v}^{\gamma s} \tag{2.29}$$

The next sections illustrate that from the above equations several well-known physical theories can be derived.

2.4. Diffusion Potential

The electric flux through the mixture is

$$\boldsymbol{i} = F \sum_{\gamma=f,+,-} \frac{\phi^\gamma z^\gamma}{\overline{V}^\gamma} \boldsymbol{v}^{\gamma s} \tag{2.30}$$

$\boldsymbol{i}$ is defined as the current electric flux through a surface of the mixture which initially equalled a unit surface. If use is made of (2.29), we find

$$\boldsymbol{i} = -F \sum_{\gamma=f,+,-} z^\gamma \sum_{\beta=f,+,-} \boldsymbol{L}^{\beta\gamma} \cdot \overline{V}^\beta \boldsymbol{\nabla}_0 \mu^\beta \tag{2.31}$$

in which $\boldsymbol{L}^{\beta\gamma}$ are the conductances:

$$\boldsymbol{L}^{\beta\gamma} = \frac{\phi^{\gamma}\phi^{\beta}(\boldsymbol{B}^{-1})^{\beta\gamma}}{\overline{V}^{\beta}\overline{V}^{\gamma}} \tag{2.32}$$

$\boldsymbol{B}^{-1}$ is the inverse of the matrix of tensors $[\boldsymbol{B}^{\beta}\gamma]_{\beta,\gamma=f,+,-}$ used in eqs. (2.28-2.29). Substituting the standard expressions for the electrochemical potentials into eq. (2.31), we find:

$$\begin{aligned} \boldsymbol{i} = & \left(-F \sum_{\gamma=f,+,-} z^{\gamma} \sum_{\beta=f,+,-} \boldsymbol{L}^{\beta\gamma} \cdot (\overline{V}^{\beta} \boldsymbol{\nabla}_0 p + RT \boldsymbol{\nabla}_0 ln a^{\beta}) \right) \\ & -\boldsymbol{L}_e \cdot \boldsymbol{\nabla}_0 \xi \end{aligned} \tag{2.33}$$

with

$$\boldsymbol{L}_e = F^2 \sum_{\gamma=f,+,-} \sum_{\beta=f,+,-} z^{\gamma} z^{\beta} \boldsymbol{L}^{\beta\gamma} \tag{2.34}$$

the electrical conductance. At uniform temperature and pressure, when $\boldsymbol{i} = \boldsymbol{0}$, the electrical potential gradient is given by:

$$-\boldsymbol{\nabla}_0 \xi = RT \sum_{\beta=f,+,-} \boldsymbol{T}^{\beta} \cdot \boldsymbol{\nabla}_0 ln a^{\beta} \tag{2.35}$$

with $\boldsymbol{T}^{\beta}$ the reduced electrical transport tensor of component β:

$$\boldsymbol{T}^{\beta} = F \boldsymbol{L}_e^{-1} \cdot \sum_{\gamma=f,+,-} z^{\gamma} \boldsymbol{L}^{\beta\gamma} \tag{2.36}$$

in analogy to the reduced electrical transport number introduced by Staverman [32]: An integrated form of (2.35) is

$$\xi_2 - \xi_1 = -RT \int_1^2 \sum_{\beta=f,+,-} [\boldsymbol{n}_0 ds_0 \cdot \boldsymbol{T}^{\beta} \cdot \boldsymbol{\nabla}_0 ln a^{\beta}] \tag{2.37}$$

in which $\boldsymbol{n}_0 ds_0$ is an infinitesimal segment of the path from 1 to 2, transformed back to the initial configuration. In the special case of a onedimensional non-deforming medium (2.37) is the classic isothermal diffusion potential derived by Nernst [28],[29] and later by Staverman [32]. Note that the uncharged water is also included in the summation.

2.5. Electrokinetic Relationships

The volume flux through the mixture is, in its Lagrangian form:

$$\boldsymbol{j} = \sum_{\gamma=f,+,-} \phi^{\gamma} \boldsymbol{v}^{\gamma s} \tag{2.38}$$

or, if use is made of (2.29) and (2.32), we find

$$\boldsymbol{j} = - \sum_{\gamma=f,+,-} \overline{V}^{\gamma} \sum_{\beta=f,+,-} \boldsymbol{L}^{\beta\gamma} \cdot \overline{V}^{\beta} \boldsymbol{\nabla}_0 \mu^{\beta} \tag{2.39}$$

Substituting the standard expressions for the electrochemical potentials into eq. (2.39), we find:

$$\boldsymbol{j} = - \sum_{\gamma=f,+,-} \overline{V}^{\gamma} \sum_{\beta=f,+,-} \boldsymbol{L}^{\beta\gamma} \cdot (F z^{\beta} \boldsymbol{\nabla}_0 \xi + RT \boldsymbol{\nabla}_0 ln a^{\beta}) - \boldsymbol{L}_p \cdot \boldsymbol{\nabla}_0 p \tag{2.40}$$

with

$$\boldsymbol{L}_p = \sum_{\gamma=f,+,-} \sum_{\beta=f,+,-} \overline{V}^{\gamma} \overline{V}^{\beta} \boldsymbol{L}^{\beta\gamma} \tag{2.41}$$

If no gradients in chemical activities are assumed, eqs. (2.33) and (2.40) reduce to electrokinetic relationships:

$$\boldsymbol{j} = -\boldsymbol{L}^{p} \cdot \boldsymbol{\nabla}_0 p - \boldsymbol{L}^{pe} \cdot \boldsymbol{\nabla}_0 \xi \tag{2.42}$$

$$\boldsymbol{i} = -\boldsymbol{L}^{pe} \cdot \boldsymbol{\nabla}_0 p - \boldsymbol{L}^{e} \cdot \boldsymbol{\nabla}_0 \xi \tag{2.43}$$

in which

$$\boldsymbol{L}^{pe} = F \sum_{\gamma=f,+,-} \sum_{\beta=f,+,-} \overline{V}^{\gamma} z^{\beta} \boldsymbol{L}^{\beta\gamma} \tag{2.44}$$

As a result of the symmetry of the eqs. (2.42) and (2.43), a threedimensional form of the four Saxen's relations can be found: one connecting streaming current to electro-osmotic pressure,

$$(\boldsymbol{j})_{\boldsymbol{\nabla}_0 \xi = \boldsymbol{0}} \cdot (\boldsymbol{\nabla}_0 p)_{\boldsymbol{j}=\boldsymbol{0}} = (\boldsymbol{i})_{\boldsymbol{\nabla}_0 \xi = \boldsymbol{0}} \cdot (\boldsymbol{\nabla}_0 \xi)_{\boldsymbol{j}=\boldsymbol{0}} \tag{2.45}$$

one connecting streaming potential and electro-osmotic flow,

$$(\boldsymbol{j})_{\boldsymbol{\nabla}_0 p = \boldsymbol{0}} \cdot (\boldsymbol{\nabla}_0 p)_{\boldsymbol{i}=\boldsymbol{0}} = (\boldsymbol{i})_{\boldsymbol{\nabla}_0 p = \boldsymbol{0}} \cdot (\boldsymbol{\nabla}_0 \xi)_{\boldsymbol{i}=\boldsymbol{0}} \tag{2.46}$$

one connecting second streaming potential and second electro-osmotic pressure

$$(\boldsymbol{j})_{\boldsymbol{i}=\boldsymbol{0}} \cdot (\boldsymbol{\nabla}_0 p)_{\boldsymbol{j}=\boldsymbol{0}} = (\boldsymbol{i})_{\boldsymbol{j}=\boldsymbol{0}} \cdot (\boldsymbol{\nabla}_0 \xi)_{\boldsymbol{i}=\boldsymbol{0}} \tag{2.47}$$

one connecting second streaming current and second electro-osmotic flow,

$$(\boldsymbol{j})_{\boldsymbol{\nabla}_0 p = \boldsymbol{0}} \cdot (\boldsymbol{\nabla}_0 p)_{\boldsymbol{\nabla}_0 \xi = \boldsymbol{0}} = (\boldsymbol{i})_{\boldsymbol{\nabla}_0 \xi = \boldsymbol{0}} \cdot (\boldsymbol{\nabla}_0 \xi)_{\boldsymbol{\nabla}_0 p = \boldsymbol{0}} \tag{2.48}$$

2.6. Reconstruction of the biphasic theory of Biot

The biphasic theory, [4], is obtained from the previous by skipping all the term relating to the presence of fixed charges and ions. Conservation of mass follows from (2.4):

$$\nabla \cdot \boldsymbol{v}^s + \nabla \cdot \left(\phi^f (\boldsymbol{v}^f - \boldsymbol{v}^s)\right) = 0 \tag{2.49}$$

Conservation of momentum is obtained by substitution of eq. (2.19) into eq. (2.13):

$$\nabla \cdot \boldsymbol{\sigma}^{eff} - \nabla p = \mathbf{0} \tag{2.50}$$

while the stress-strain relationship is given by (2.23)

$$\boldsymbol{\sigma}^{eff} = \frac{1}{J} \boldsymbol{F} \cdot \frac{\partial W}{\partial \boldsymbol{E}} \cdot \boldsymbol{F}^c \tag{2.51}$$

in which the strain energy function W depends only on local deformation. Darcy's law follows from eqs. (2.29) and (2.22):

$$\phi^f \boldsymbol{v}^{fs} = -\boldsymbol{K} \cdot \nabla_0 (p + \frac{\partial W}{\partial \Phi^f}) \tag{2.52}$$

in which the term $\frac{\partial W}{\partial \Phi^f}$ is interpreted for immiscible mixtures as the matric potential. Equations (2.49-2.52) are the biphasic equations.

2.7. Recapitulation

2.7.1. The equations

In short, the quadriphasic equations are as follows:
The momentum balance of the mixture (2.13) in which we substitute eq. (2.19) :

$$\nabla \cdot \boldsymbol{\sigma}_e - \nabla p = \mathbf{0} \tag{2.53}$$

The mass balance of the mixture (2.4) :

$$\nabla \cdot \boldsymbol{v}^s - \nabla \cdot \phi^f (\boldsymbol{v}^f - \boldsymbol{v}^s) = 0 \tag{2.54}$$

The mass balance of the ionic constituents (2.6):

$$\frac{D^s \Phi^\alpha}{Dt} + J \nabla \cdot [\phi^\alpha (\boldsymbol{v}^\alpha - \boldsymbol{v}^s)] = 0 \quad \alpha = +, - \tag{2.55}$$

The reversible constitutive relationships (2.23) :

$$\boldsymbol{\sigma}_e = (\det \boldsymbol{F})^{-1} \boldsymbol{F} \cdot \frac{\partial W}{\partial \boldsymbol{E}^s} \cdot \boldsymbol{F}^c \tag{2.56}$$

and (2.22)

$$\begin{aligned} \mu^f &= \frac{\partial W}{\partial \Phi^f} + p \\ \mu^+ &= \frac{\partial W}{\partial \Phi^+} + p + \frac{\lambda}{V^+} \\ \mu^- &= \frac{\partial W}{\partial \Phi^-} + p - \frac{\lambda}{V^-} \end{aligned} \tag{2.57}$$

The dissipative constitutive relationships, containing Darcy's law and Fick's law (2.29) :

$$-\phi^\beta \nabla_0 \mu^\beta = \sum_{\gamma=f,+,-} \boldsymbol{B}^{\beta\gamma} \cdot \boldsymbol{v}^{\gamma s} \tag{2.58}$$

The incompressibility of the solid :

$$(1 - \phi^f) \det \boldsymbol{F} = 1 - \phi_0^f \tag{2.59}$$

The fixation of the fixed charges to the solid (2.9) :

$$\phi^f c^{fc} \det \boldsymbol{F} = \phi_0^f c_0^{fc} \tag{2.60}$$

The reversible constitutive relationships are described by one function : the strain energy function W. The dissipative constitutive relationships are described by a symmetric semi-positive definite matrix $\boldsymbol{B}$. W depends on the deformation of the solid, the volume fraction of the fluid Φ^f, cations Φ^+ and anions Φ^-. Equation (2.54) says that the volume change of the porous solid, expressed as the divergence of the solid velocity $\boldsymbol{v}^s$, is caused by in or outflow of fluid. This flux depends in turn on the gradients of chemical potential of the fluid, and of the electrochemical potentials of the ions according to eq. (2.58).

Equations (2.55) are the mass balance of cations and anions, in which the relative ionic velocities $\boldsymbol{v}^\alpha - \boldsymbol{v}^s = \boldsymbol{F} \cdot \boldsymbol{v}^{\alpha s}$ are expressed as a function of gradients of (electro)chemical potentials by eqs. (2.58) .

2.7.2. Boundary conditions

As for single-phase materials momentum balance of the boundary is compulsory:

$$[(\boldsymbol{\sigma}_e - p\boldsymbol{I}) \cdot \boldsymbol{n}] = \boldsymbol{0} \tag{2.61}$$

with $\boldsymbol{n}$ de outer normal along the boundary. From eqs (2.58) we can infer that the following jump conditions should hold along the boundary :

$$[\bar{V}^f \mu^f] = 0 \tag{2.62}$$

$$[\bar{V}^+ \mu^+] = 0 \tag{2.63}$$

$$[\bar{V}^- \mu^-] = 0 \tag{2.64}$$

because the fluxes across the boundary cannot be infinite .

2.8. Example of a constitutive relationship

We take the example of a material complying with linear isotropic elasticity and Donnan-osmosis (Fig. 2). In this case the strain energy function W takes the form :

$$\begin{aligned} W = \; & \mu_O{}^f N^f + \mu_0{}^+ N^+ + \mu_0{}^- N^- - RT\Gamma \left(\tfrac{N^+}{V^+} + \tfrac{N^-}{V^-}\right) ln(N^f) + \\ & + RT \tfrac{N^+}{V^+} \left(ln \tfrac{f^+ N^+}{V^+} - 1\right) + \\ & + RT \tfrac{N^-}{V^-} \left(ln \tfrac{f^- N^-}{V^-} - 1\right) + \tfrac{\lambda_s}{2} tr\boldsymbol{E} tr\boldsymbol{E} + \mu_s \boldsymbol{E} : \boldsymbol{E} \end{aligned} \tag{2.65}$$

in which Γ is the osmotic coefficient, f^+ the activity coefficient of the cations, f^- the activity coefficient of the anions, λ_s and μ_s the Lamé constants. From eqs. (2.56) and (2.57) we derive expressions for the stress and the (electro) chemical potentials :

$$\boldsymbol{\sigma}_e = \tfrac{1}{J} \boldsymbol{F} \cdot (\lambda_s \boldsymbol{I} tr\boldsymbol{E} + 2\mu \boldsymbol{E}) \cdot \boldsymbol{F}^c \tag{2.66}$$

$$\mu^f = \mu_0{}^f(T) + p - RT\Gamma(c^+ + c^-) \tag{2.67}$$

$$\mu^+ = \mu_0{}^+(T) + p + \tfrac{RT}{V^+} ln \tfrac{f^+ N^+}{V^+ (N^f)^\Gamma} + \tfrac{\lambda}{V^+} \tag{2.68}$$

$$\mu^- = \mu_0{}^-(T) + p + \tfrac{RT}{V^-} ln \tfrac{f^- N^-}{V^- (N^f)^\Gamma} - \tfrac{\lambda}{V^-} \tag{2.69}$$

In eq. (2.67) we identify the chemical potential in the same way as in section 1. It is the difference between the mechanical pressure p and the osmotic pressure π given by eq. (1.64). The eqs. (2.68-2.69) are consistent with the expression (1.41) for the limiting case of a dilute solution ($\Gamma \to 1$ and $f^{\beta} \to 1$).

3. Multiporosity model for blood perfusion

A multiporosity description of finite deformation of a porous solid is developed using the theory of mixtures. Unlike existing multiporosity models from the literature this formulation includes anisotropy of interfaces between porosities. Each porosity is dealt with as a separate component. Fluid flow between porosities are mass exchange term between components. Rather than accounting for a discrete number of porosities a continuous spectrum of intercommunicating compartments is introduced. Conservation laws for mass and momentum have been derived and additionally appropriate formulations for the constitutive behaviour of the constituents are proposed. A finite element description of the hierarchical mixture model has been implemented. 2-D, axi-symmetric and 3-D elements can be used in finite deformation analysis. An example of application is blood perfused biological tissue. A simulation of a blood perfused contracting skeletal muscle is presented.

3.1. Introduction

In this theory the various solid and fluid components of the tissue are modelled as interacting continua. An important fluid component in biological tissue is blood. It is responsible for the nutrition and drainage processes that are essential for the tissue. Blood flows through a hierarchical system of blood vessels: the vascular tree. This tree consists of one or a few large arterial vessels from which smaller vessels bifurcate and diverge into numerous capillaries which assemble to converging venous vessels. Because of this hierarchical architecture blood flow cannot be adequately described by biphasic mixture theory: the state of the blood strongly depends on the position in the hierarchy. For example, the velocity and pressure of the capillary blood are much lower than of the arterial blood. The pressure difference between arterial and venous vessels is essential as the driving force for the blood flow. Huyghe *et al.* (1989) developed an extended form of Darcy's equation in which this dependency of the fluid flow on hierarchical

position was included. In addition the hydraulic permeability matrices are shown to be related quantitatively to the microstructure of the vessel tree of the tissue.

They verified this relationship for Newtonian flow through a rigid vascular tree [22, 21, 41]. Because in biological tissue alterations in blood perfusion can occur due to deformations of the tissue [12], the focus of this section is to illustrate the concepts developed in [22] into a finite deformation theory of saturated porous media. Aifantis (1977) introduced the concept of multiporosity for deforming media that are characterized by several distinct families of flow paths. A special case of this concept, in which only two degrees of diffusivity were included, was applied to fissured rock formations, in which most of the fluid volume is located in the low hydraulic permeability pores of the rock, and most of the hydraulic permeability is associated with the fissures [44]. Two different types of permeabilities are included in these models : one is an intracompartmental hydraulic permeability involving flow within a compartment, the other is intercompartmental hydraulic permeability involving flow between compartments. In the present approach mixed terms between intra- and intercompartmental hydraulic permeability occur in addition to those occuring in Aifantis [1]. These mixed terms account for anisotropy of the interface between compartments. In other words, Aifantis [1] implicitly assume the interfaces to be isotropically oriented. The tissue is modelled as a mixture of one solid and one fluid where the fluid represents the blood. The fluid is subdivided into a number of compartments, each of which represents the blood on a different hierarchical position in the vascular tree. Blood flow through the vasculature is described as communication between the fluid compartments, which corresponds with the physiological definition of perfusion: the volume of blood passing a given level in the vascular hierarchy per unit of time and per volume of tissue. Vessel walls, modelled as an elastic solid-fluid interface, are included as a local contribution of the pressure difference between solid and fluid to the mixture's elastic energy. Although this mixture description is specifically developed for biological materials, its applicability to technical materials is not excluded.

In the derivation of the mixture model conservation laws of mass and momentum have been formulated and corresponding constitutive behaviour has been derived from constitutive theory [40]. Elsewhere the same finite deformation multiporosity equations are derived through averaging of a Poiseuille-type pressure flow relationship at the level of the individual blood vessel [23, 24].

An integrated finite element description of the total mixture model has been developed and implemented in the DIANA software package [5]. The implementation was subjected to several test procedures, one of which was comparison of the finite element solution with the analytical solution for a confined compression test [38]. As an illustration of the possibilities of the model a simulation of contraction of a perfused skeletal muscle is performed. Further examples of computations are found in the literature, including 3D analyses [39], comparison with animal experiments [42] and a model study [43].

3.2. Conservation Laws

In technical literature we find porous media theories dealing with solids saturated with different fluid constituents [3]. Bowen (1980) has derived equations from mixture theory for ν incompressible immiscible fluids saturating one incompressible solid. The equations of conservation of mass are formulated for each constituent and in case of intrinsic incompressibility of each constituent, their quasi-static local form can be denoted as:

$$\frac{\partial \phi^\alpha}{\partial t} + \nabla \cdot (\phi \alpha \boldsymbol{v}^\alpha) = \theta^\alpha \quad , \quad \alpha = 1, \ldots, \nu \tag{3.1}$$

in which θ^α is the volume transfer from constituent α to the other constituents. Assuming no volume loads and no inertia, the balance of momentumreads :

$$\nabla \cdot \boldsymbol{\sigma}^\alpha + \boldsymbol{\pi}^\alpha = \mathbf{0} \quad , \quad \alpha = 1, \ldots, \nu \tag{3.2}$$

where ϕ^α is the volume fraction, $\boldsymbol{v}^\alpha$ the velocity, $\boldsymbol{\sigma}^\alpha$ the Cauchy stress tensor and $\boldsymbol{\pi}^\alpha$ are the momentum interaction of constituent α with other constituents. The exponent α refers to the constituent number and t is time. Balance of mass for the total mixture requires:

$$\sum_\alpha \theta^\alpha = 0. \tag{3.3}$$

Likewise for the balance of momentum:

$$\sum_\alpha \boldsymbol{\pi}^\alpha = \mathbf{0}. \tag{3.4}$$

Furthermore no moment of momentum interaction between the constituents is assumed, so that $\boldsymbol{\sigma}^{\alpha}$ is symmetric.

A hierarchical mixture can be thought of to consist of one solid constituent and a fluid constituent that is divided into a continuous series of fluid compartments. Each fluid compartment resides on a specific position in the hierarchy of pores of the solid. The fluid in a compartment flows spatially through the solid (spatial flow) and communicates with compartments on neighbouring hierarchical positions (hierarchical flow). The position in the hierarchy is quantified by a dimensionless parameter x_0, which is assumed to run from 0 to 1, and the communication between the fluid compartments is described by the fluid volume interaction term θ^f appearing in Eq. (3.1). A fluid compartment defined by the hierarchical range $[x_0, x_0 + dx_0]$ has a volume fraction $\tilde{\phi}^f dx_0$ in which $\tilde{\phi}^f$ represents the fluid volume fraction per unit hierarchical parameter x_0. Generally in this paper a tilde will be used to indicate that a quantity depends on x_0 and, if the quantity is volume specific, is defined per unit x_0. The exponents s and f refer to solid and fluid, respectively. The mass balance for one fluid compartment is:

$$\frac{\partial \tilde{\phi}^f}{\partial t} dx_0 + \boldsymbol{\nabla} \cdot (\tilde{\phi}^f \tilde{\boldsymbol{v}}^f) dx_0 = \tilde{\phi}^f_{(x_0)} \tilde{v}^f_{0(x_0)} - \tilde{\phi}^f_{(x_0+dx_0)} \tilde{v}^f_{0(x_0+dx_0)} \tag{3.5}$$

in which the right hand side represents the volume interaction with the neighbouring compartments. $\tilde{v}^f_0$ is a measure of the rate at which fluid flows from one compartment to the next, and is defined as the material time derivative of x_0 with respect to the fluid:

$$\tilde{v}^f_0 = \frac{D^f x_0}{Dt} \,. \tag{3.6}$$

It can be shown that $\tilde{\phi}^f \tilde{v}^f_0$ corresponds to the traditional, physiological definition of regional blood perfusion [11, 22]. Dividing Eq. (3.5) by dx_0 yields for infinitesimal dx_0 the local fluid mass balance:

$$\frac{\partial \tilde{\phi}^f}{\partial t} + \boldsymbol{\nabla} \cdot (\tilde{\phi}^f \tilde{\boldsymbol{v}}^f) = \tilde{\theta}^f = -\frac{\partial (\tilde{\phi}^f \tilde{v}^f_0)}{\partial x_0} \,. \tag{3.7}$$

Assuming no mass interaction between solid and fluid, the mass balance for the total mixture (3.3) is rewritten:

$$\theta^s = \int_0^1 \tilde{\theta}^f dx_0 = 0 \,. \tag{3.8}$$

Because the actual hierarchical fluid volume fraction $\tilde{\phi}^f$ is defined per unit x_0, saturation of the mixture is expressed as:

$$\phi^s + \int_0^1 \tilde{\phi}^f dx_0 = \phi^s + \phi^f = 1 \,, \tag{3.9}$$

which can be used in combination with Eqs. (3.7) and (3.8) to rewrite solid, fluid and total mass conservation as:

$$-\frac{\partial \phi^f}{\partial t} + \nabla \cdot ((1-\phi^f)\boldsymbol{v}^s) = 0 \tag{3.10}$$

$$\frac{\partial \tilde{\phi}^f}{\partial t} + {}_4\nabla \cdot (\tilde{\phi}^f \, {}_4\tilde{\boldsymbol{v}}^f) = 0 \tag{3.11}$$

$$\nabla \cdot ((1-\phi^f)\boldsymbol{v}^s) + \int_0^1 ({}_4\nabla \cdot (\tilde{\phi}^f \, {}_4\tilde{\boldsymbol{v}}^f)) dx_0 = 0 \,, \tag{3.12}$$

where ${}_4\nabla$ is a four-dimensional operator and ${}_4\tilde{\boldsymbol{v}}^f$ a four-dimensional vector:

$${}_4\nabla = \begin{bmatrix} \frac{\partial}{\partial x_0} \\ \nabla \end{bmatrix}, \qquad {}_4\tilde{\boldsymbol{v}}^f = \begin{bmatrix} \tilde{v_0}^f \\ \tilde{\boldsymbol{v}}^f \end{bmatrix} . \tag{3.13}$$

Because the fluid related quantities depend on x_0, the momentum balance of the total mixture is written as:

$$\nabla \cdot \boldsymbol{\sigma}^s + \int_0^1 \nabla \cdot \tilde{\boldsymbol{\sigma}}^f dx_0 = \mathbf{0} \tag{3.14}$$

where the balance condition for momentum interaction, Eq. (3.4), has been used:

$$\boldsymbol{\pi}^s + \int_0^1 \tilde{\boldsymbol{\pi}}^f dx_0 = \mathbf{0}. \tag{3.15}$$

3.3. Constitutive Laws

In the derivation of requirements for the constitutive behaviour the first and second laws of thermodynamics are used. The first law, conservation of

total energy, reads - under quasi-static conditions - for constituent α of a unit volume of mixture :

$$\dot{U}^\alpha = \dot{W}^\alpha + \dot{Q}^\alpha + \dot{E}^\alpha \tag{3.16}$$

where U^α is the total internal energy, W^α is the external work, Q^α is the heat supply of phase α and E^α is the energy gain of α due to interaction. The dots above the variables denote their material time derivatives. Assuming intrinsic incompressibility and quasi-stationarity for each constituent, Eq. (3.16) can be written for the solid and fluid constituents in a volume V of mixture with surrounding surface A:

$$\begin{aligned}
&\frac{\partial}{\partial t}\left(\int_V \phi^s U^s \, dV\right) + \int_A \phi^s U^s \boldsymbol{v}^s \cdot \boldsymbol{n} \, dA = \int_A \boldsymbol{v}^s \cdot \boldsymbol{\sigma}^s \cdot \boldsymbol{n} \, dA + \\
&\int_V \phi^s r^s \, dV + \int_A \boldsymbol{h}^s \cdot \boldsymbol{n} \, dA + \int_V \epsilon^s \, dV + \int_V \boldsymbol{\pi}^s \cdot \boldsymbol{v}^s \, dV \, , \qquad (3.17) \\
&\frac{\partial}{\partial t}\left(\int_V \tilde{\phi}^f \tilde{U}^f \, dV\right) + \int_A \tilde{\phi}^f \tilde{U}^f \tilde{\boldsymbol{v}}^f \cdot \boldsymbol{n} \, dA + \int_V \frac{\partial}{\partial x_0}(\tilde{\phi}^f \tilde{U}^f \tilde{v}_0^f) \, dV = \\
&\int_A \tilde{\boldsymbol{v}}^f \cdot \tilde{\boldsymbol{\sigma}}^f \cdot \boldsymbol{n} \, dA + \int_V \frac{\partial}{\partial x_0}(\tilde{v}_0^f \tilde{\sigma}_0^f) \, dV + \int_V \tilde{\phi}^f \tilde{r}^f \, dV + \int_A \tilde{\boldsymbol{h}}^f \cdot \boldsymbol{n} \, dA + \\
&\int_V \frac{\partial}{\partial x_0}(\tilde{h}_0^f) \, dV + \int_V \tilde{\epsilon}^f \, dV + \int_V \tilde{\boldsymbol{\pi}}^f \cdot \tilde{\boldsymbol{v}}^f \, dV \, , \qquad (3.18)
\end{aligned}$$

where r^α is the internal heat supply, $\boldsymbol{h}^\alpha$ the external heat supply and ϵ^α the direct energy supply of constituent α due to interaction. $\tilde{\sigma}_0^f$ is the fluid stress at the interface between neighbouring hierarchical levels and h_0^f the heat supply between neighbouring hierarchical levels. Note that Eq. (3.18) is expressed per unit of x_0, and that internal energy variation of the fluid due to volume interaction is included in the third term. Applying Gauss' theorem gives for the local conservation of total energy of the solid and the fluid:

$$\begin{aligned}
&\frac{\partial}{\partial t}(\phi^s U^s) = -\boldsymbol{\nabla} \cdot (\phi^s U^s \boldsymbol{v}^s) + \boldsymbol{\nabla} \cdot (\boldsymbol{v}^s \cdot \boldsymbol{\sigma}^s) + \phi^s r^s + \\
&\qquad \boldsymbol{\nabla} \cdot \boldsymbol{h}^s + \epsilon^s + (\boldsymbol{\pi}^s \cdot \boldsymbol{v}^s) \, , \qquad (3.19) \\
&\frac{\partial}{\partial t}(\tilde{\phi}^f \tilde{U}^f) = -\boldsymbol{\nabla} \cdot (\tilde{\phi}^f \tilde{U}^f \tilde{\boldsymbol{v}}^f) - \frac{\partial}{\partial x_0}(\tilde{\phi}^f \tilde{U}^f \tilde{v}_0^f) + \boldsymbol{\nabla} \cdot (\tilde{\boldsymbol{v}}^f \cdot \tilde{\boldsymbol{\sigma}}^f) + \\
&\frac{\partial}{\partial x_0}(\tilde{v}_0^f \tilde{\sigma}_0^f) + \tilde{\phi}^f \tilde{r}^f + \boldsymbol{\nabla} \cdot \tilde{\boldsymbol{h}}^f + \frac{\partial}{\partial x_0}(\tilde{h}_0^f) + \tilde{\epsilon}^f + \tilde{\boldsymbol{\pi}}^f \cdot \tilde{\boldsymbol{v}}^{f\,\prime}, \qquad (3.20)
\end{aligned}$$

which is rewritten using the material time derivative of U, and the local mass and momentum balances Eqs. (3.10) and (3.11):

$$\phi^s \frac{D^s U^s}{Dt} = \boldsymbol{\sigma}^s : (\boldsymbol{\nabla} \boldsymbol{v}^s) + \phi^s r^s + \boldsymbol{\nabla} \cdot \boldsymbol{h}^s + \epsilon^s \,, \tag{3.21}$$

$$\tilde{\phi}^f \frac{D^f \tilde{U}^f}{Dt} =$$

$$\tilde{\boldsymbol{\sigma}}^f : (\boldsymbol{\nabla} \tilde{\boldsymbol{v}}^f) + \frac{\partial}{\partial x_0}(\tilde{\sigma}_0^f \tilde{v}_0^f) + \tilde{\phi}^f \tilde{r}^f + {}_4\boldsymbol{\nabla} \cdot {}_4\tilde{\boldsymbol{h}}^f + \tilde{\epsilon}^f . \tag{3.22}$$

In Eq. (3.22) we made use of the four-dimensional gradient operator ${}_4\boldsymbol{\nabla}$ and fluid velocity ${}_4\tilde{\boldsymbol{v}}^f$ (Eq. (3.13)) and the analogously defined external heat supply ${}_4\tilde{\boldsymbol{h}}^f$:

$${}_4\tilde{\boldsymbol{h}}^f = \begin{bmatrix} \tilde{h}_0^f \\ \tilde{\boldsymbol{h}}^f \end{bmatrix} . \tag{3.23}$$

The local balance condition of the energy interaction of the mixture requires that no energy is created by the interaction:

$$\epsilon^s + \boldsymbol{\pi}^s \cdot \boldsymbol{v}^s + \int_0^1 (\tilde{\epsilon}^f + \tilde{\boldsymbol{\pi}}^f \cdot \tilde{\boldsymbol{v}}^f) dx_0 = 0 \,. \tag{3.24}$$

The second law of thermodynamics, the entropy inequality, is introduced:

$$dS \geq \frac{dQ}{T} \tag{3.25}$$

which relates the change of entropy of the mixture, dS, to the supplied heat dQ at a temperature T. For a volume V of mixture with surrounding surface A and constant temperature T in each constituent this is written as:

$$\begin{aligned} &\frac{\partial}{\partial t}\Big(\int_V \phi^s S^s \, dV\Big) + \int_A \phi^s S^s \boldsymbol{v}^s \cdot \boldsymbol{n} \, dA + \int_0^1 \Big[\frac{\partial}{\partial t}\Big(\int_V \tilde{\phi}^f \tilde{S}^f \, dV\Big) + \\ &\int_A \tilde{\phi}^f \tilde{S}^f \tilde{\boldsymbol{v}}^f \cdot \boldsymbol{n} \, dA + \int_V \frac{\partial}{\partial x_0}(\tilde{\phi}^f \tilde{S}^f \tilde{v}_0^f) \, dV\Big] dx_0 \geq \\ &\int_V \frac{\phi^s r^s}{T} \, dV + \int_A \frac{\boldsymbol{h}^s \cdot \boldsymbol{n}}{T} \, dA + \\ &\int_0^1 \Big[\int_V \frac{\tilde{\phi}^f \tilde{r}^f}{T} \, dV + \int_A \frac{\tilde{\boldsymbol{h}}^f \cdot \boldsymbol{n}}{T} \, dA + \int_V \frac{\partial}{\partial x_0}\Big(\frac{\tilde{h}_0^f}{T}\Big) \, dV\Big] dx_0 \,. \end{aligned} \tag{3.26}$$

By applying Gauss' theorem and making use of the material time derivative of S, the local form of Eq. (3.26) can be written as:

$$\phi^s \frac{D^s S^s}{Dt} + \int_0^1 (\tilde{\phi}^f \frac{D^f \tilde{S}^f}{Dt}) dx_0 \geq$$
$$\frac{1}{T}(\phi^s r^s + \nabla \cdot \boldsymbol{h}^s + \int_0^1 (\tilde{\phi}^f \tilde{r}^f + {}_4\nabla \cdot {}_4\tilde{\boldsymbol{h}}^f) dx_0) \,. \tag{3.27}$$

Substituting the local energy equations for solid and fluid, Eqs. (3.21) and (3.22), into the local entropy inequality, Eq. (3.27), yields:

$$\phi^s \frac{D^s S^s}{Dt} + \int_0^1 (\tilde{\phi}^f \frac{D^f \tilde{S}^f}{Dt}) dx_0 \geq \frac{1}{T}(\phi^s \frac{D^s U^s}{Dt} - \boldsymbol{\sigma}^s : (\nabla \boldsymbol{v}^s) + \boldsymbol{\pi}^s \cdot \boldsymbol{v}^s$$
$$+ \int_0^1 [\tilde{\phi}^f \frac{D^f \tilde{U}^f}{Dt} - \tilde{\boldsymbol{\sigma}}^f : (\nabla \tilde{\boldsymbol{v}}^f) - \frac{\partial}{\partial x_0}(\tilde{\sigma}_0^f \tilde{v}_0^f) + \tilde{\boldsymbol{\pi}}^f \cdot \tilde{\boldsymbol{v}}^f] dx_0) \tag{3.28}$$

in which the total energy interaction $\epsilon^s + \int_0^1 \tilde{\epsilon}^f dx_0$ was eliminated by means of Eq. (3.24). Introducing Helmholtz' free energy $F = U - TS$ for each constituent, and substituting momentum balance Eq. (3.14) yields:

$$\frac{1}{T}(-\phi^s \frac{D^s F^s}{Dt} + \boldsymbol{\sigma}^s : (\nabla \boldsymbol{v}^s) + \boldsymbol{v}^s \cdot (\nabla \cdot \boldsymbol{\sigma}^s) + \int_0^1 [-\tilde{\phi}^f \frac{D^f \tilde{F}^f}{Dt} +$$
$$\tilde{\boldsymbol{\sigma}}^f : (\nabla \tilde{\boldsymbol{v}}^f) + \tilde{\boldsymbol{v}}^f \cdot (\nabla : \tilde{\boldsymbol{\sigma}}^f) + \frac{\partial}{\partial x_0}(\tilde{\sigma}_0^f \tilde{v}_0^f)] dx_0) \geq 0 \,. \tag{3.29}$$

Expressing Eq. (3.29) per unit of undeformed volume of mixture and transforming the material time derivative of F^f yields:

$$-J\phi^s \frac{D^s F^s}{Dt} + J\nabla \cdot (\boldsymbol{\sigma}^s \cdot \boldsymbol{v}^s) + \int_0^1 [-J\tilde{\phi}^f \frac{D^s \tilde{F}^f}{Dt} +$$
$$J\ {}_4\nabla \cdot ({}_4\tilde{\boldsymbol{\sigma}}^f \cdot {}_4\tilde{\boldsymbol{v}}^f) - J\tilde{\phi}^f ({}_4\tilde{\boldsymbol{v}}^f - {}_4\boldsymbol{v}^s) \cdot {}_4\tilde{\nabla}\tilde{F}^f] dx_0 \geq 0 \,. \tag{3.30}$$

For compactness of notation, the four-dimensional fluid stress tensor ${}_4\tilde{\boldsymbol{\sigma}}^f$ and solid velocity vector ${}_4\boldsymbol{v}^s$ have been used, which is written in matrix notation:

$${}_4\tilde{\boldsymbol{\sigma}}^f = \begin{bmatrix} \tilde{\sigma}_0^f & \mathbf{0} \\ \mathbf{0} & \tilde{\boldsymbol{\sigma}}^f \end{bmatrix} \quad ; \quad {}_4\boldsymbol{v}^s = \begin{bmatrix} 0 \\ \boldsymbol{v}^s \end{bmatrix} \,. \tag{3.31}$$

Again rewriting the material time derivatives of F gives:

$$-\frac{D^s J\phi^s F^s}{Dt} + F^s \frac{D^s J\phi^s}{Dt} + J\nabla\cdot(\boldsymbol{\sigma}^s\cdot\boldsymbol{v}^s) + \int_0^1 [-\frac{D^s J\tilde{\phi}^f \tilde{F}^f}{Dt} +$$
$$\tilde{F}^f \frac{D^s J\tilde{\phi}^f}{Dt} - J\tilde{\phi}^f({}_4\tilde{\boldsymbol{v}}^f - {}_4\boldsymbol{v}^s)\cdot {}_4\nabla\tilde{F}^f + J\ {}_4\nabla\cdot({}_4\tilde{\boldsymbol{\sigma}}^f\cdot {}_4\tilde{\boldsymbol{v}}^f)]dx_0$$
$$\geq 0\,. \tag{3.32}$$

Because of incompressibility of the solid, $\frac{D^s(J\phi^s)}{Dt} = 0$. Substituting the Lagrangian form of the equation of conservation of fluid mass (Eq. (3.11)):

$$\frac{D^s(J\tilde{\phi}^f)}{Dt} + J\ {}_4\nabla\cdot(\tilde{\phi}^f({}_4\tilde{\boldsymbol{v}}^f - {}_4\boldsymbol{v}^s)) = 0 \tag{3.33}$$

in Eq. (3.32) yields:

$$\int_0^1 [-\frac{D^s\tilde{W}}{Dt} + J\nabla\cdot(\boldsymbol{\sigma}^s\cdot\boldsymbol{v}^s) - \tilde{F}^f J\ {}_4\nabla(\tilde{\phi}^f({}_4\tilde{\boldsymbol{v}}^f - {}_4\boldsymbol{v}^s)) -$$
$$J\tilde{\phi}^f({}_4\tilde{\boldsymbol{v}}^f - {}_4\boldsymbol{v}^s)\cdot {}_4\nabla\tilde{F}^f + J\ {}_4\nabla\cdot({}_4\tilde{\boldsymbol{\sigma}}^f\cdot {}_4\tilde{\boldsymbol{v}}^f)]dx_0 \geq 0\,, \tag{3.34}$$

where the strain energy function $\tilde{W} = J\phi^s F^s + J\tilde{\phi}^f\tilde{F}^f$ has been introduced. By using the total stress defined as $\boldsymbol{\sigma} = \boldsymbol{\sigma}^s + \int_0^1 \tilde{\boldsymbol{\sigma}}^f dx_0$, Eq. (3.34) can be written as:

$$J\boldsymbol{\sigma} : (\nabla\boldsymbol{v}^s) + \int_0^1 [-\frac{D^s\tilde{W}}{Dt} - J\ {}_4\nabla\cdot(\tilde{\phi}^f({}_4\tilde{\boldsymbol{v}}^f - {}_4\boldsymbol{v}^s)\tilde{F}^f) +$$
$$J\nabla\cdot((\,{}_4\tilde{\boldsymbol{v}}^f - {}_4\boldsymbol{v}^s)\cdot {}_4\tilde{\boldsymbol{\sigma}}^f)]dx_0 \geq 0\,. \tag{3.35}$$

Expressing the free energy of the fluid per unit mixture volume as $\tilde{\psi}^f = \tilde{\phi}^f\tilde{F}^f$, introducing the well known effective stress $\boldsymbol{\sigma}^{eff} = \boldsymbol{\sigma} + p\boldsymbol{I}$ [33] and adding the total mass balance Eq. (3.12) with a Lagrange multiplier p, Eq. (3.35) can be written as:

$$J\boldsymbol{\sigma}^{eff} : (\nabla\boldsymbol{v}^s) + \int_0^1 [-\frac{D^s\tilde{W}}{Dt} +$$
$$J({}_4\tilde{\boldsymbol{\sigma}}^f - \tilde{\psi}^f\,{}_4\boldsymbol{I} - p\tilde{\phi}^f\,{}_4\boldsymbol{I}) : {}_4\nabla({}_4\tilde{\boldsymbol{v}}^f - {}_4\boldsymbol{v}^s) +$$
$$J({}_4\tilde{\boldsymbol{v}}^f - {}_4\boldsymbol{v}^s)\cdot({}_4\nabla\cdot {}_4\tilde{\boldsymbol{\sigma}}^f - {}_4\nabla\tilde{\psi}^f + p\ {}_4\nabla\tilde{\phi}^f)]dx_0 \geq 0 \tag{3.36}$$

where ${}_4\boldsymbol{I}$ represents the four-dimensional unity tensor. We choose as independent variables the Green-Lagrange strain tensor $\boldsymbol{E}$, the Lagrangian

form of the fluid volume fraction $J\tilde{\phi}^f$ and the relative velocity ${}_4\tilde{\boldsymbol{v}}^{fs} = {}_4\boldsymbol{F}^{-1} \cdot ({}_4\tilde{\boldsymbol{v}}^f - {}_4\boldsymbol{v}^s)$. For convenience of notation we introduced the four-dimensional tensor $\boldsymbol{F}$:

$$\boldsymbol{F} = \begin{bmatrix} 1 & \boldsymbol{0} \\ \boldsymbol{0} & \boldsymbol{F} \end{bmatrix}, \tag{3.37}$$

in which $\boldsymbol{F}$ is the deformation tensor. Applying the principle of equipresence and the chain rule for time differentiation of $\tilde{W}$ and defining $W = \int_0^1 \tilde{W} dx_0$, yields the inequality:

$$\begin{aligned} [J\boldsymbol{\sigma}^{eff} - \boldsymbol{F} \cdot \frac{\partial W}{\partial \boldsymbol{E}} \cdot \boldsymbol{F}^c] : \boldsymbol{\nabla} \boldsymbol{v}^s + \int_0^1 [& - \frac{\partial \tilde{W}}{\partial\, {}_4\tilde{\boldsymbol{v}}^{fs}} \cdot \frac{D^s\, {}_4\tilde{\boldsymbol{v}}^{fs}}{Dt} \\ & + J({}_4\tilde{\boldsymbol{\sigma}}^f + (\tilde{\mu}^f \tilde{\phi}^f - \tilde{\psi}^f)\, {}_4\boldsymbol{I}) : {}_4\boldsymbol{\nabla}({}_4\tilde{\boldsymbol{v}}^f - {}_4\boldsymbol{v}^s) \\ & + J({}_4\tilde{\boldsymbol{v}}^f - {}_4\boldsymbol{v}^s) \cdot (-{}_4\boldsymbol{\nabla}\tilde{\psi}^f + \tilde{\mu}^f\, {}_4\boldsymbol{\nabla}\tilde{\phi}^f + \\ & {}_4\boldsymbol{\nabla} \cdot {}_4\tilde{\boldsymbol{\sigma}}^f)] dx_0 \geq 0 \end{aligned} \tag{3.38}$$

which should be true for any value of the state variables. The definition of the chemical potential of the fluid

$$\tilde{\mu}^f = \frac{\partial \tilde{W}}{\partial (J\tilde{\phi}^f)} + p \,. \tag{3.39}$$

has been used in Ineq. (3.38). The fourth term of the left-hand side of Ineq. (3.38) represents the dissipation due to fluid flow. The first term is linear in the solid velocity gradient, the second linear in the accelerations and the third linear in the relative velocity gradients. Therefore, by a standard argument, we find the constitutive relations:

$$\boldsymbol{\sigma}^{eff} = \tfrac{1}{J} \boldsymbol{F} \cdot \frac{\partial W}{\partial \boldsymbol{E}} \cdot \boldsymbol{F}^c \tag{3.40}$$

$$\frac{\partial \tilde{W}}{\partial\, {}_4\tilde{\boldsymbol{v}}^{fs}} = {}_4\boldsymbol{0} \tag{3.41}$$

$${}_4\tilde{\boldsymbol{\sigma}}^f = (\tilde{\psi}^f - \tilde{\mu}^f \tilde{\phi}^f)\, {}_4\boldsymbol{I} \tag{3.42}$$

leaving as inequality:

$$\begin{aligned} J \int_0^1 [& ({}_4\tilde{\boldsymbol{v}}^f - {}_4\boldsymbol{v}^s) \cdot (-{}_4\boldsymbol{\nabla}\tilde{\psi}^f + \\ & \tilde{\mu}^f\, {}_4\boldsymbol{\nabla}\tilde{\phi}^f + {}_4\boldsymbol{\nabla} \cdot {}_4\tilde{\boldsymbol{\sigma}}^f)] dx_0 \geq 0 \,. \end{aligned} \tag{3.43}$$

If we assume that dissipation associated with fluid flow is a quadratic function of the fluid velocities we find:

$$-{}_4\nabla_0\tilde{\psi}^f + \tilde{\mu}^f\,{}_4\nabla_0\tilde{\phi}^f + {}_4\nabla_0 \cdot {}_4\tilde{\boldsymbol{\sigma}}^f = {}_4\tilde{\boldsymbol{B}}^f \cdot {}_4\tilde{\boldsymbol{v}}^{fs} \,. \tag{3.44}$$

Substituting the constitutive expression Eq. (3.42) of the fluid stress ${}_4\tilde{\boldsymbol{\sigma}}^f$ into Eq. (3.44), yields the extended Darcy equation:

$$-\tilde{\phi}^f\,{}_4\nabla_0\tilde{\mu}^f = {}_4\tilde{\boldsymbol{B}}^f \cdot {}_4\tilde{\boldsymbol{v}}^{fs} \tag{3.45}$$

which can be written in a more common form [22]:

$$\tilde{\phi}^f\,{}_4\tilde{\boldsymbol{v}}^{fs} = -{}_4\tilde{\boldsymbol{K}} \cdot {}_4\nabla_0\tilde{\mu}^f \tag{3.46}$$

in which the four-dimensional hydraulic permeability tensor ${}_4\tilde{\boldsymbol{K}}$ reads:

$${}_4\tilde{\boldsymbol{K}} = (\tilde{\phi}^f)^2\,{}_4\tilde{\boldsymbol{B}}^{f^{-1}} = \begin{bmatrix} \tilde{k}_{00} & \tilde{\boldsymbol{k}}_0 \\ \tilde{\boldsymbol{k}}_0 & \tilde{\boldsymbol{K}} \end{bmatrix} \tag{3.47}$$

and which is consistent with earlier forms derived by formal averaging [24].

3.4. Numerical Implementation

The hierarchical mixture model has been implemented in the finite element software package DIANA. The displacement of the solid $\boldsymbol{u}^s$, the hydrostatic pressure p and the fluid pressure $\tilde{\mu}^f$ have been chosen as the degrees of freedom. Three equations are used: 1 the momentum balance (3.2), in which the constitutive equation for the effective stress (3.40) is substituted, 2 the solid mass balance (3.10), and 3 the fluid mass balance (3.11), in which the extended Darcy equation (3.46) is substituted. The weighted residual method has been applied to the resulting system of non-linear coupled differential equations. After spatial discretization of the degrees of freedom the weighting functions are chosen according to Galerkin's method. Special attention was paid to the discretization of the fluid pressure $\tilde{\mu}^f$, which depends on both spatial position $\boldsymbol{x}$ and x_0. Its spatial discretization was achieved analogously to the hydrostatic pressure's discretization, while an extra linear discretization in x_0 direction was used. A more detailed description of the finite element formulation and implementation is given

in [38]. The resulting total element matrix equation is:

$$\begin{bmatrix} 0 & 0 & 0 \\ {}^{u}_{s}B^{JL}_{j} & {}^{p}_{s}B^{JM} & {}^{\mu^f}_{s}B^{JN}_{n} \\ 0 & {}^{p}_{f}B^{KM}_{k} & {}^{\mu^f}_{f}B^{KN}_{kn} \end{bmatrix} \begin{bmatrix} \delta\dot{u}^{L}_{j} \\ \delta\dot{p}^{M} \\ \delta\dot{\tilde{\mu}}^{fN}_{n} \end{bmatrix} + \begin{bmatrix} {}^{u}_{m}K^{IL}_{ij} & {}^{p}_{m}K^{IM}_{i} & 0 \\ 0 & 0 & 0 \\ 0 & 0 & {}^{\mu^f}_{f}K^{KN}_{kn} \end{bmatrix} \begin{bmatrix} \delta u^{L}_{j} \\ \delta p^{M} \\ \delta\tilde{\mu}^{fN}_{n} \end{bmatrix} = \begin{bmatrix} {}_{m}R^{I}_{exi} \\ 0 \\ {}_{f}R^{K}_{exk} \end{bmatrix} - \begin{bmatrix} {}_{m}R^{I}_{ini} \\ {}_{s}R^{J}_{in} \\ {}_{f}R^{K}_{ink} \end{bmatrix} \tag{3.48}$$

with:
δu^{L}_{j}: iterative correction of displacement component in direction j of node L,
δp^{M}: iterative correction of hydrostatic pressure in node M,
$\delta\tilde{\mu}^{fN}_{n}$: iterative correction of fluid pressure at hierarchical level n in node N.
and a dot above a variable denotes its material time derivative. In this matrix equation symmetry is found in the submatrices ${}^{p}_{s}\boldsymbol{B}$, ${}^{\mu^f}_{f}\boldsymbol{B}$, ${}^{u}_{m}\boldsymbol{K}$, ${}^{\mu^f}_{f}\boldsymbol{K}$ and moreover ${}^{p}_{f}B^{KM}_{k} = {}^{\mu^f}_{s}B^{MK}_{k}$ and ${}^{u}_{s}B^{JL}_{j} = {}^{p}_{m}K^{LJ}_{j}$. Thus a fully symmetric matrix equation is obtained after time integration of the damping contribution. This time integration is achieved by a third order Houbolt scheme [2]:

$$\dot{s}(t) = h_0 s(t) + \sum_{i=1}^{3} h_i s(t-\tau_i) \quad ; \quad s = \boldsymbol{u}^s, p, \tilde{\mu}^f \ . \tag{3.49}$$

Linear and quadratic two-dimensional, axi-symmetric and three-dimensional isoparametric elements of the serendipity family can be used [34]. The non-linear equations can be solved by several regular and modified Newton-Raphson iteration techniques and a direct Gauss decomposition [35]. The implementation has been tested for several problems. Rigid body rotations and translations and analytical solutions of a one-dimensional confined compression experiment and a four-dimensional Laplace equation have been succesfully computed [38].

3.5. Application

A simulation of a perfusion experiment on an isometrically (at constant length) and tetanically (sustained) contracting skeletal muscle has been performed, using the finite element model. The muscle under consideration is a rat calf muscle (gastrocnemius medialis), of which the geometry has been roughly estimated from experimental measurements. This muscle is about 30 mm long and 6 mm thick. The mesh consists of 112 6-node wedge-shaped 3-D elements for the muscle belly, 22 3-node triangular plane stress elements for each aponeurosis and 2 3-node triangular plane stress elements for each tendon. The tendons and aponeuroses, tendinous sheets on the muscle surface, attach the tendons to the muscle belly. The tendons, each consisting of 2 triangular 3-node plane stress elements, and the aponeuroses, each consisting of 22 similar elements, are isotropic and linearly elastic, with a Young modulus of 1.5 10^6 kPa [36] and Poisson ratio of 0.3. The thickness of the tendons is 0.5 mm. The thickness of the aponeuroses runs from 0.5 mm at the tendon to 0.01 mm at the other end.

The passive material behaviour of the muscle tissue is based on a transverse isotropic, non-linearly elastic description of cardiac tissue according to Bovendeerd (1990). The direction of anisotropy (e_1) corresponds with the direction of the muscle fibers , and the contribution of the local Green strain in the tissue to the elastic energy is:

$$W_E = C[e^{a(2E_{11}^2+E_{22}^2+E_{33}^2+2E_{12}^2+2E_{23}^2+2E_{31}^2)} - 1] \tag{3.50}$$

where $C = 0.7$ kPa, $a = 5.0$. The elastic energy is assumed to depend also on strain in vessel walls, which is associated with changes in vascular volume. The contribution of the vessel strain to the elastic energy is expressed as:

$$W_C = \frac{1}{2\tilde{c}}(J\tilde{\phi}^f)^2 \tag{3.51}$$

where the vessel compliance $\tilde{c}$ represents the relation between the local blood volume fraction and local intra-extra vascular pressure difference:

$$\tilde{c} = \frac{\partial(J\tilde{\phi}^f)}{\partial(\tilde{\mu}^f - p)} \ . \tag{3.52}$$

The values for $\tilde{c}$ that were used in the simulation are listed in Table 1. Thus

the total strain energy function of the muscle material reads:

$$\begin{aligned} W &= W_E + W_C \\ &= C\left[e^{a(2E_{11}^2+E_{22}^2+E_{33}^2+2E_{12}^2+2E_{23}^2+2E_{31}^2)} - 1\right] + \frac{1}{2\tilde{c}}(J\tilde{\phi}^f)^2 \end{aligned} \quad (3.53)$$

Contraction is described as an active second Piola-Kirchhoff stress component in fiber direction depending on time:

$$s_f = \frac{S_{max}}{\lambda_f}\left(1 - \left(\frac{1}{(1+(\frac{t}{t_r})^4)}\right)\right) \quad (3.54)$$

where $S_{max} = 100$ kPa, λ_f is the relative elongation in fiber direction, $t_r = 0.05$ s, and t is time (s). This contraction function is a rough approximation of the stress generation in tetanic contraction of rat gastrocnemius medialis muscle.

	$\tilde{K}\ (\frac{mm^2}{s\ kPa})$	$\tilde{k}_{00}\ (\frac{1}{s\ kPa})$	$\tilde{c}(\frac{1}{kPa})$
arterial	100	0.0025	0.001
arteriolar	0.05	0.00025	0.01
venular	0.02	0.0025	0.1

Table 1: Blood perfusion parameters.

Discretization of the hierarchical range is achieved by 3 linear segments, resulting in arterial, arteriolar, capillary and venous blood pressures in each spatial nodal point. The vascular segments are assumed to represent the arterial bed, arteriolar bed and the capillary-venous bed respectively.

The hydraulic permeability tensor ${}_4\tilde{\boldsymbol{K}}$ and the vessel compliance $\tilde{c}$ are prescribed for each compartment according to table 1, whereas they are constant in the whole geometry. For the sake of simplicity ${}_4\tilde{\boldsymbol{K}}$, which is defined according to eq. (3.47), is diagonal, where $\tilde{\boldsymbol{K}} = \tilde{K}\boldsymbol{I}$. We assume that the main artery and vein penetrate into the muscle at the tip of one of the aponeuroses. At that position the nodal arterial input pressure is set at 10 kPa, and nodal venous outflow pressure at 0 kPa. No force load is applied to the muscle. Due to these nodal boundary conditions a stationary blood flow pattern is reached after about 0.3 s.

In Fig. 4a,b,c contours of arterial, capillary and venous blood pressures are given. Also hierarchic capillary flow (volume averaged blood flow through the

capillary compartment, which corresponds to the physiological definition of regional capillary perfusion, defined as volume of blood passing the capillaries per second and per volume of tissue) is given in Fig. 4d. The calculated values approximate experimentally measured values, which were found to be circa 2.5 10^{-3} s^{-1} in resting skeletal muscle [13].

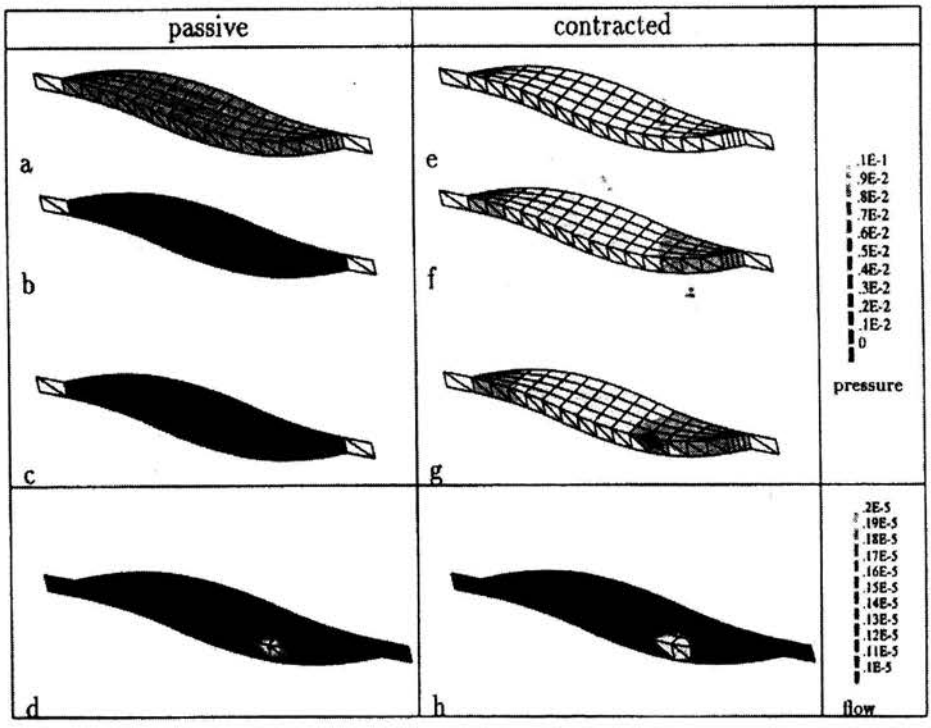

Figure 4: Contours of blood pressures (MPa) and hierarchical flows (1/ms) in passive and contracting muscle. a: passive arterial blood pressure. b: passive capillary blood pressure. c: passive venous blood pressure. d: passive hierarchic capillary flow. e: arterial blood pressure during contraction. f: capillary blood pressure during contraction. g: venous blood pressure during contraction. h: hierarchic capillary flow during contraction.

When the muscle is in the stationary perfusion state, contraction is started. After 0.1 s the contraction stress has reached its maximum value. Due to the contraction, a significant rise in intramuscular pressure (hydrostatic pressure in the solid) occurs, which is transmitted to the blood via the elastic vessel walls. The arterial blood pressure slightly increases (Fig. 4e). Capillary

and venous pressure however, increase drastically (Fig. 4f,g).
Moreover we find a strongly decreased hierarchical flow for the capillary blood (Fig. 4h), which is due to the decreased pressure difference between the capillary and venous compartments.

3.6. Discussion

Finite element analysis often aims at predicting failure of structures. Whereas failure of technical materials is mostly associated with excess of stress, biological material often fails due to disturbance of the supply of nutrients and drainage of waste matter. Finite element analysis of technical structures therefore focusses on stress analysis, whereas finite element analysis of biological structures ought to persue a broader scope of mechanical function, including remodelling processes and transport phenomena. Regional capillary perfusion, being a key quantity for transport through many biological tissues, we believe is essential to include as a field variable in the analysis of mechanical function of biological tissues. Moreover, tissue deformation and blood perfusion are mechanically linked [27, 30]. The model presented in this paper, specifically describes the mechanical interaction between blood perfusion and deformation of the tissue, and as such may provide a better insight in this interaction.

In the simulation it is shown that in an isometrically contracting skeletal muscle, the rise in intramuscular pressure is transferred particularly to the capillary and venous blood compartments, which results in a decrease of the capillary flow (regional capillary perfusion), which is consistent with experiments reported in [45].

The hydraulic permeability tensor ${}_4\tilde{\boldsymbol{K}}$ contains much information about vessel distribution, vessel directions and vessel density for each compartment and each mesh-element. Because no values for ${}_4\tilde{\boldsymbol{K}}$ were available, it was made diagonal for the sake of simplicity. However, values for ${}_4\tilde{\boldsymbol{K}}$ can be derived from geometrical information of a vascular tree [22, 21, 41]. This information can for example be obtained by reconstruction of the vasculature by corrosion casting. For the large arterial and venous vessels, the vessel density of the tissue is very low and inhomogeneous which makes them relatively easy to reconstruct. Accurate simulation of the perfusion in these compartments however might need special attention, because the model deals with volume averaged quantities, which intrinsically assume homogeneity within the averaging volume. For the largest vessels a discrete approach may

offer a better accuracy. On the other hand the small vessels like arterioles and capillaries, which are tedious to reconstruct because of their huge density, can be described rather well by the volume averaged relations of the model. Today's techniques of X-ray micro computer tomography, offers an efficient measuring method of the 3D structure of the microvasculature of any tissue. The resolution achieved by this method is probably sufficient for all but the capillary level.

References

1. AIFANTIS, E. C., *Multiporosity theories*, Developments in Mechanics, **8**, p. 209, 1977.
2. BATHE, K. J., *Finite element procedures in engineering analysis*, Prentice Hall Inc, Englewood Cliffs, New Jersey, first edition, iSBN: 0-13-317305-4, 1982.
3. BEDFORD, A. and DRUMHELLER, D. S., *Theories of immiscible and structured mixtures*, Int. J. Engng Sci., **21**(8), pp. 863–960, 1983.
4. BIOT, M. A., *Theory of finite deformations of porous solids*, Indiana University Mathematics J, **21**(7), pp. 597–620, 1972.
5. BORST, R. D., KUSTERS, G., NAUTA, P. and WITTE, F. D., *DIANA - A comprehensive, but flexible finite element system.*, in C. Brebbia, ed., *Finite element systems: a handbook*, Springer Verlag, Berlin, New York and Tokyo, 1985.
6. BOVENDEERD, P. H. M., *The mechanics of the normal and ischemic left ventricle during the cardiac cycle*, PhD dissertation, University of Limburg, Department of Biophysics, 1990.
7. BOWEN, R. M., *Incompressible porous media models by use of the theory of mixtures*, Int. J. Engng Sci., **18**, pp. 1129–1148, 1980.
8. CHANG, R., *Physical chemistry with applications to biological systems*, MacMillan Publishing Co., Inc., New York, 2 edition, iSBN: 0-02-979050-X, 1981.
9. DE HEUS, H. J., *Verification of mathematical models describing soft charged hydrated tissue behaviour*, PhD dissertation, Eindhoven University of Technology, Department of Mechanical Engineering, 1994.
10. FRIJNS, A., HUYGHE, J. and JANSSEN, J., *A validation of the quadriphasic mixture theory for intervertebral disc tissue*, Int. J. Eng. Sci., **35**, pp. 1419–1429, 1997.
11. GUYTON, A. C., *Textbook of medical physiology*, W.B. Saunders Company, Philadelphia, 7th edition, 1986.
12. HOFFMAN, J. I. E. and SPAAN, J. A. E., *Pressure-flow relations in coronary circulation*, Physiol.Rev., **70**(2), pp. 331–90, 1990.

13. HUDLICKA, O., TYLER, K. R., WRIGHT, A. J. A. and ZIADA, A. M. A. R., *Growth of capillaries in skeletal muscles*, in F. Hammersen and K. Messmer, eds., *Skeletal muscle microcirculation; Proceedings of the 3rd Bodensee Symposium on Microcirculation*, number 5 in Progress in Applied Microcirculation, Karger, Basel, pp. 44–61, 1984.

14. HUYGHE, J., *Intra-extrafibrillar mixture formulation of soft charged hydrated tissues*, Journal of Theoretical and Applied mechanics, **37**(3), pp. 519–536, 1999.

15. HUYGHE, J., HOUBEN, G., DROST, M. and VAN DONKELAAR, C., *An ionisedńon-ionised dual porosity model of intervertebral disc tissue: experimental quantification of parameters.*, Biomechanics and modelling in mechanobiology, **2**, pp. 3–19, 2003.

16. HUYGHE, J., JANSSEN, C., VAN DONKELAAR, C. and LANIR, Y., *Measuring principles of frictional coefficients in cartilaginous tissues and its substitutes*, Biorheology, **39**, pp. 47–53, 2002.

17. HUYGHE, J. and JANSSEN, J., *Quadriphasic mechanics of swelling incompressible porous media*, Int. J. Eng. Sci., **35**, pp. 793–802, 1997.

18. HUYGHE, J. and JANSSEN, J., *Thermo-chemo-electro-mechanical formulation of saturated charged porous solids*, Transport in Porous Media, **34**, pp. 129–141, 1999.

19. HUYGHE, J. M. and BOVENDEERD, P. H. M., *Biological mixtures*, Polish Academy of Sciences, Warschau, Poland, 2003.

20. HUYGHE, J. M., JANSSEN, C., LANIR, Y., VAN DONKELAAR, C., MAROUDAS, A. and VAN CAMPEN, D., *Experimental measurement of elctrical conductivity and electro-osmotic permeability of ionised porous media*, in W. Ehlers and J. Bluhm, eds., *Porous media: theoretical, experimental and numerical applications*, Springer Verlag, Berlin, Germany, pp. 295–313, 2002.

21. HUYGHE, J. M., OOMENS, C. W. and VAN CAMPEN, D. H., *Low Reynolds number steady state flow through a branching network of rigid vessels: II. A finite element mixture model*, Biorheology, **26**, pp. 73–84, 1989.

22. HUYGHE, J. M., OOMENS, C. W., VAN CAMPEN, D. H. and HEETHAAR, R. M., *Low Reynolds number steady state flow through a branching network of rigid vessels: I. A mixture theory*, Biorheology, **26**, pp. 55–71, 1989.

23. HUYGHE, J. M. and VAN CAMPEN, D. H., *Finite deformation theory of hierarchically arranged porous solids: I. Balance of mass and momentum*, Int. J. Engng Sci., **33**(13), pp. 1861–1871, 1995.

24. HUYGHE, J. M. and VAN CAMPEN, D. H., *Finite deformation theory of hierarchically arranged porous solids: II. Constitutive behaviour*, Int. J. Engng Sci., **33**(13), pp. 1873–1886, 1995.

25. KATCHALSKY, A. and CURRAN, P., *Nonequilibrium thermodynamics in biophysics*, Harvard University Press, Cambridge, Ma, U.S.A., 1965.

26. LANIR, Y., SEYBOLD, J., SCHNEIDERMAN, R. and HUYGHE, J. M., *Partition and diffusion of sodium and chloride ions in soft charged foam : the effect of external salt concentration and mechanical deformation*, Tissue Engineering, **4**(4), pp. 365–378, 1998.

27. LIVINGSTON, J. Z. and RESAR, J. R., *Effect of tetanic myocardial contraction on coronary pressure-flow relationships*, Am.J.Physiol., **265**, pp. H1215–H1226, 1993.

28. NERNST, W., *Zur Kinetik der in Loesung befindlichen Koerper.*, Z. Phys. Chem., **2**, pp. 613–637, 1888.

29. NERNST, W., *Die electromotorische Wirksamkeit der Jonen.*, Z. Phys. Chem., **4**, pp. 129–181, 1889.

30. RESAR, J. R., JUDD, R. M., HALPERIN, H. R., CHACKO, V. P., WEISS, R. G. and YIN, F. C. P., *Direct evidence that coronary perfusion affects diastolic myocardial mechanical properties in canine heart*, Cardiovasc.Res., **27**, pp. 403–410, 1993.

31. RICHARDS, E. G., *An introduction to the physical properties of large molecules in solution*, Cambridge University Press, Cambridge, 1 edition, iSBN: 0-521-23110-8, 1980.

32. STAVERMAN, A. J., *Non-equilibrium thermodynamics of membrane processes.*, Trans. Faraday Soc., **48**, pp. 176–185, 1952.

33. TERZAGHI, K., *Theoretical soil mechanics*, John Wiley and Sons, New York, 1943.

34. TNO, *DIANA User's Manual: Linear Static Analysis*, TNO Building and Construction Research, Delft, The Netherlands, release 5.1, vol. 1, 1993.

35. TNO, *DIANA User's Manual: Non-linear Analysis*, TNO Building and Construction Research, Delft, The Netherlands, release 5.1, vol. 4, 1993.

36. TRESTIK, C. L. and LIEBER, R. L., *Relationship between Achilles tendon mechanical properties and gastrocnemius muscle function*, J. Biomech. Eng., **115**(3), pp. 225–30, 1993.

37. VAN LOON, R., HUYGHE, J., WIJLAARS, M. and BAAIJENS, F., *3D FE implementation of an incompressible quadriphasic mixture model*, Int. J. Numer. Meth. Engng., in press, 2003.

38. VANKAN, W. J., HUYGHE, J. M., DROST, M. R., JANSSEN, J. D. and HUSON, A., *A finite element mixture model for hierarchical porous media*, Int. J. Num. Meth. Eng., **40**, pp. 193–210, 1997.

39. VANKAN, W. J., HUYGHE, J. M., JANSSEN, J. D. and HUSON, A., *A 3-D finite element model of blood perfused rat gastrocnemius medialis muscle*, Eur. J. Morphology, **34**(1), pp. 19–24, 1996.

40. VANKAN, W. J., HUYGHE, J. M., JANSSEN, J. D. and HUSON, A., *Poroelasticity of saturated solids with an application to blood perfusion*, Int. J. Engng Sci., **34**(9), pp. 1019–1031, 1996.

41. VANKAN, W. J., HUYGHE, J. M., JANSSEN, J. D., HUSON, A., HACKING, W. J. G. and SCHREINER, W., *Finite element analysis of blood flow through biological tissue*, Int. J. Engng Sci., **35**, pp. 375–385, 1997.

42. VANKAN, W. J., HUYGHE, J. M., SLAAF, D. W., VAN DONKELAAR, C. C., DROST, M. R., JANSSEN, J. D. and HUSON, A., *A finite element model of blood perfusion in muscle tissue during compression and sustained contraction*, Am. J. Physiol., **273**, pp. H1587–H1594, 1997.

43. VANKAN, W. J., HUYGHE, J. M., VAN DONKELAAR, C. C., DROST, M. R., JANSSEN, J. D. and HUSON, A., *Mechanical blood–tissue interaction in contracting muscles: a model study*, J. Biomechanics, **31**, pp. 401–409, 1998.

44. WILSON, R. K. and AIFANTIS, E. C., *On the theory of consolidation with double porosity*, Int. J. Engng Sci., **20**(9), pp. 1009–1035, 1982.

45. WISNES, A. and KIRKEBØ, A., *Regional distribution of blood flow in calf muscles of rat during passive stretch and sustained contraction*, Acta Physiol. Scand., **96**, pp. 256–266, 1976.